Seismic Microzonation of the Pompeii Archaeological Park (Southern Italy): Local Seismic Amplification Factors

Vincenzo Amato, Marina Covolan, Hélène Dessales, Alfonso Santoriello

geosciences

MDPI

Article

Seismic Microzonation of the *Pompeii* Archaeological Park (Southern Italy): Local Seismic Amplification Factors

Vincenzo Amato [1,2,*], Marina Covolan [3,4,*], Hélène Dessales [5] and Alfonso Santoriello [4]

[1] Department of Bioscience and Territory, University of Molise, Contrada Fonte Lappone, 86090 Pesche, Italy
[2] Applied Research Laboratory, *Pompeii* Archaeological Park, Via Plinio, 26, 80045 Pompei, Italy
[3] Centre Jean Bérard UAR 3133 CNRS, EfR, Via Francesco Crispi, 86, 80121 Napoli, Italy
[4] Department of Cultural Heritage Sciences, University of Salerno, Via Giovanni Paolo II, 132, 84084 Fisciano, Italy; asantori@unisa.it
[5] AOROC UMR 8546 Laboratory, ENS-EPHE, CNRS-Université PSL, 45 Rue d'Ulm, 75005 Paris, France; helene.dessales@ens.psl.eu
* Correspondence: vincenzo.amato@unimol.it (V.A.); mmcovolan@gmail.com (M.C.)

Abstract: Pompeii Archaeological Park is the best laboratory for the study of the seismic site effects on cultural heritage: the ancient site was destroyed and buried by the 79 AD Vesuvian eruption and, furthermore, it was also affected by the 62–63 AD strong earthquake. Large sectors of the city were reconstructed after this earthquake while other parts were still under reconstruction when the fall-out and pyroclastic density currents of the eruption buried the Roman city. In order to evaluate the distribution of the damage and reconstructions due to the earthquake, detailed mappings of the structures were carried out using multidisciplinary approaches. In addition, analyses of the topographical features, subsoil stratigraphies, and geophysical surveys, responsible for local seismic amplification (site effects), allow us to define the sectors of the ancient city where the Amplification Factors (AFs) were the main ones responsible for damage. Selected areas and examples of compromised and reconstructed buildings show that the ancient topography and subsoil features (both lithological and seismic) are the main AFs. In particular, the damages caused by the 62–63 AD earthquakes seem to be mainly due to topographical factors such as steep scarps and slopes, ridges, peaks, and terraces, as well as to the major thickness of the soft sediments (loose volcanoclastic layers, paleosols, weathered lavas, and anthropogenic infillings) located over the well-lithified lavas. It is not uncommon to also have the combination of these two factors. For the first time, this multidisciplinary approach allows us to draw a seismic microzonation map for one of the most important archaeological sites of the world.

Keywords: seismic hazard; risk mitigation; cultural heritage; earthquakes; geomorphology; stratigraphy

Citation: Amato, V.; Covolan, M.; Dessales, H.; Santoriello, A. Seismic Microzonation of the *Pompeii* Archaeological Park (Southern Italy): Local Seismic Amplification Factors. *Geosciences* **2022**, *12*, 275. https://doi.org/10.3390/geosciences12070275

Academic Editors: Hans-Balder Havenith and Jesus Martinez-Frias

Received: 3 June 2022
Accepted: 4 July 2022
Published: 8 July 2022

1. Introduction

From the beginning of the 20th century, there has been an improvement in studies concerning the significant role of the local geological–geomorphological setting in controlling the distribution of damage induced by earthquakes [1–3]. Several theoretical models based on experimental data highlighted the relationships between ground shaking and geological–geomorphological settings. They are responsible for seismic energy trapping and resonance phenomena in the shallowest part of the subsurface and relative interference phenomena of engineering interest [4]. Starting from these approaches, the international community, e.g., [5,6], adopted seismic codes to evaluate the ground motion amplification phenomena in order to elaborate the anti-seismic planning of new structures and to preserve the archaeological cultural heritage. These codes distinguish between

seismic hazard assessments on a regional scale and at the local level: the first is assessed by considering the seismogenic processes and regional-scale radiation patterns of earthquakes; the second by examining the modifications induced on the ground shaking at small-scale (tens to hundreds of meters) geological–geomorphological settings. These modifications are estimated by numerical models that account for the seismo-stratigraphical and geotechnical model of the local subsoil, e.g., [4]. The parameterization of these models (in terms of Vp and Vs profiles) also takes into consideration borehole data and/or surface geophysical measurements, e.g., [7,8], as well as having application in well-known case-study tests [9–14].

The strategies developed under the denomination of seismic microzonation (hereinafter SM) are devoted to seismic hazard assessment at the scale of the settlement and surrounding land (typically in urban areas). SM requires a strongly multidisciplinary approach, which takes advantage of the full interoperability between geological/geomorphological surveys, archaeological and architectural data, geophysical prospections, models, and testing. This approach requires a coherent methodological workflow among geologists, geophysicists, archaeologists, geotechnical engineers, and, ultimately, land planners.

The Italian scientific community (coordinated within the Centre for Seismic Microzonation and Applications, https://www.centromicrozonazionesismica.it/en/ accessed on 11 June 2021, under the coordination of the Civil Protection Department) developed specific guidelines for SM studies [15–17]. Moreover, SM includes three levels of investigation.

Level 1 is based on the collection and reinterpretation of previous data concerning shallow subsurface (i.e., borehole data, geological/geomorphological surveys, geotechnical, and geophysical data) [18] combined with field surveys and geomorphological analysis of detailed scale topographic maps (1:5000). The geological–geomorphological model is drawn after reclassification of the geological units into SM units following their geotechnical properties [19,20]. This model subdivides the study area in homogeneous parcels of land (seismically homogenous microzones (SHM)), each characterized by similar expected co-seismic phenomena. Despite the inherently semi-qualitative character of the SM first level, its outcomes are of primary importance for the subsequent levels.

Level 2 represents an in-depth analysis that allows the identification of areas with high uncertainties where further investigations are needed in order to define a SM, which in turn derives from the combination of the previous SHM with the numerical quantification of the local seismic amplification. The latter is quantified by means of schedules (which varies for all the regions of the Italian territory, taking into account their seismotectonic and geological settings) that define the amplification factors of elastic spectra at the surface.

Finally, Level 3 consists of the planning and realization of new geological, geotechnical, and geophysical investigations in order to define the seismic site response as areas prone to local seismic amplification and/or unstable areas [8,21,22].

Despite the fact that the first-level SM is only based on geological and geomorphological field data integrated with the collection of both borehole and geophysical investigations, it can be very useful to a first definition of areas prone to local seismic amplification, and it is preparatory for the planning of the second and the third levels of investigation.

In this paper, we present and discuss the results of the collected and reinterpreted geological (mainly by borehole and archaeological trench data), geomorphological, and geophysical investigations useful for the characterization of the SM of Pompeii Archaeological Park. Three main steps are defined for the characterization of Level 1 of the SM: (a) the combination of geological/geomorphological analyses to develop a subsoil geological model and a geomorphological map of the study area (SGM and GM, respectively); (b) an upgraded model (geological/geophysical model (GGM)), by considering data provided by geophysical prospecting; and (c) the definition of a SHM map based on GGM.

In addition, an innovative and original approach was carried out in order to give useful information to plan further investigations for the second and third levels of SM. This approach takes into account both the available historical–archaeological data for the sectors of the ancient town mostly damaged by the 62–63 AD earthquake, and new archaeological data and surveys on buildings buried by the 79 AD Vesuvian eruption. In particular, the inventory of the damaged buildings was improved, adding the buildings that were restored in 79 AD, probably as consequence of the damage of the 62–63 AD earthquake. In this way, a map of the damage and restorations (damage/rebuilding map (DRM)) was intersected with the SHM map, allowing us the enhancing of a strong correlation between damage distribution and site effects. Finally, the work suggests several sectors of the ancient town where further investigations are needed at the second and third levels of SMZ.

2. Materials and Methods

The methodological workflow is based upon the following steps (Figure 1).

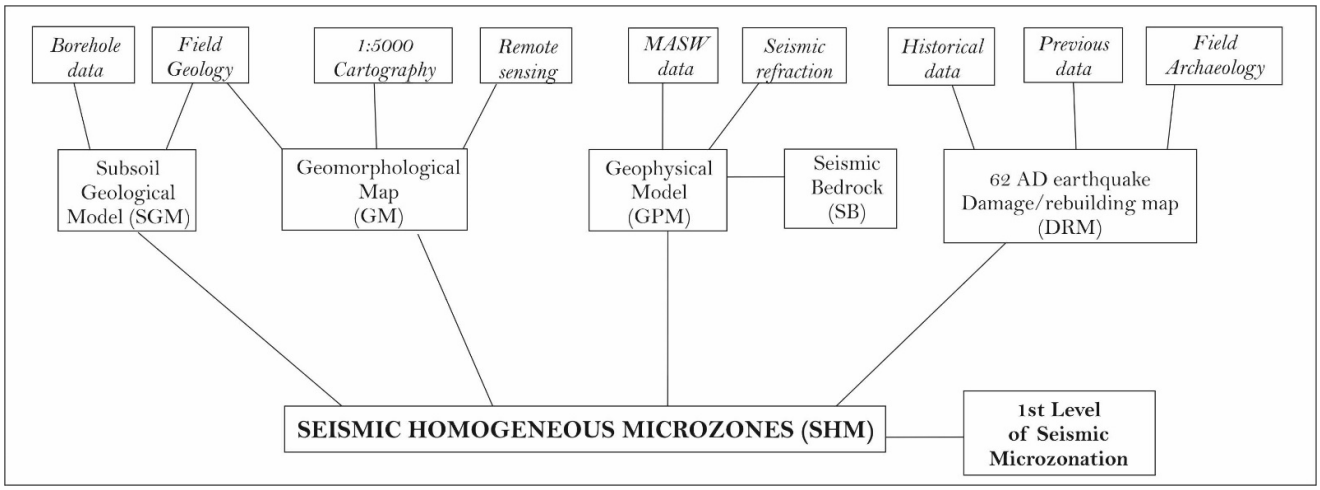

Figure 1. Workflow of the materials and methods and related products used for the drawing of the Pompeii seismic microzonation.

2.1. Subsoil Geological Model (SGM) and Geomorphological Map (GM)

The first approach concerns the definition of the zones characterized by homogeneous lithostratigraphical and geomorphological settings, including the definition of representative lithostratigraphical logs and their geometrical relationships. In this evaluation the definition of the thickness ranges of the lithostratigraphical layers is relevant for geometrical relationships, sensu ASTM [19] and CTMS [18]. SGM is represented by a map made of polygons classified as bedrock (B) and cover terrains (CTs). Bedrock is made of coherent and lithified lava of the Pompeii volcano [23] unconformably buried under CTs. The last are made by loose deposits constituted by alternating tephra layers, buried soils, and colluvial and anthropogenic layers; therefore, they have extremely variable lateral extension and thickness. This variability is due to the presence of buried morphologies carved into the bedrock or due to the anthropogenic changes of the ground level through time. In terms of seismic behavior, the sharper impedance contrast responsible for the main possible resonance phenomena is expected at the boundary between CTs and B, the latter represented by more rigid material. In this first step, by the modelling of lithostratigraphical cross-sections, it is possible to identify the occurrence of different lithostratigraphical settings or logs, expressed by the number of stacked layers, each represented in terms of (a) their belonging to the bedrock or CT; (b) type of geological units according to conventional classification, e.g., [19]; and (c) thickness range.

Therefore, the SGM is a map where any polygon corresponds to a preliminary SHM, characterized by the same subsurface lithostratigraphical setting and differs from a classic geological map where only the surface geology is represented.

New field data (ca. 100 boreholes and archaeological trenches) were added to the GIS database and supported by a detailed geomorphological study based on DEM elaborations of 1:5000 topographical and geodetical data. This study also highlights the sectors of the ancient town characterized by landforms that can enhance local seismic amplification, such as isolated peaks, ridges, scarps, steep slopes, impluvium, anthropogenic fills, channels, and underground caves, according to guidelines for SM studies [15–17].

2.2. Geophysical Model (GPM)

In this phase, the aims are twofold. First, new field data corresponding to surface geophysical prospecting were carried out in order to provide further constraints to the geometries of the lithological bodies delineated in the SGM. Second, these measurements will provide the seismic characterization of each lithostratigraphic unit present in the subsoil, in terms of Vp and Vs values. The main concern will also be the identification of the main seismic impedance contrasts and of the identification of the seismic bedrock (SB). All these elements play a major role in assessing the local seismic hazard. SB represents the bottom of the seismo-stratigraphic log responsible for the expected ground motion amplification. The SB may or may not correspond to the bedrock, depending on its characteristic V values. In fact, for engineering purposes, SB is conventionally defined with Vs values above any threshold (>800 m/s in Italy). This definition implies that, depending on the geological characteristics and history, not all bedrocks are seismic bedrocks and eventually also CTs can be SB.

This phase allows the reassessment of representative lithostratigraphical logs for each polygon of the SGM map, where the vertical sequence of geological units is delineated with a more refined thickness estimate (integrating geological and geophysical observations) along with the respective V values.

The seismic characterization of each lithostratigraphic units present in the subsoil, in terms of Vp and Vs values, was established by four seismostratigraphical tomographies (seismic refraction) and seven Multichannel Analysis of Surface Waves (MASW). The geophysical investigations are based on the measurement of the arrival times of the seismic waves refracted by the interfaces between soil stratifications, characterized by different propagation speeds. The energy source is represented by an impact on the surface. The energy radiates from the "shot point", travelling both directly in the uppermost layer (direct arrivals) and travelling deep down and laterally along layers at a higher velocity (refracted arrivals), and then returning to the surface, where it is measured through the spreading of geophones. Energizing at different positions on the surface, it will be possible to deduce information about the geometry of the deep refractor layer, in many cases coinciding with the bedrock. The seismic refraction was carried out using P.A.S.I. GEA24 complete with GEA-PC acquisition software. GEA24 is a compact-sized 24-channel seismograph with a 24-bit data acquisition board and USB interface for external PC.

The MASW surveys were carried out using a 24-bit and 24-channel MAE A6000-S 24 high-resolution seismograph. A 6 kg hammer that strikes on a circular aluminum plate was used as the seismic source. A vertical geophone (14 Hz Geospace), localized close to the plate, was used as trigger/starter. For the seismic elaboration, the source was localized to the beginning and to the end of the geophonic line, 2 m spaced, in order to obtain a seismic profile both directly and in reverse. The total length of the seismic profile ranges between 30 and 50 m, sufficiently to obtain 2D seismostratigraphy units to a maximum depth of ca. 30 m. The seismic signals were successively elaborated using SurfSeis 2.05 software of the Kansas Geological Survey.

2.3. Assessment of Damage/Rebuilding Map (DRM)

During the last decades some studies were carried out to better identify damage and reconstructions in relation with earthquakes in several worldwide urban contexts, both for recent and past earthquakes [24–37]. For the Pompeii Archeological Park, the available data on the effects of the past earthquakes on buildings are still partially lacking. Only data from historical fonts (see Section 3.1) and publications [34,38–51] are nowadays available. More recently, other important data derived from the project RECAP have been made available (*Reconstruire après un séisme. Expériences antiques et innovations à Pompéi*; http://recap.huma-num.fr/ accessed on 15 April 2022) [34,51,52], in which new approaches to the construction techniques and to the study of the building material are correlated to the seism of 62–63 AD and to the following earthquakes. The systematic and interdisciplinary research carried out during this project, in particular in the East part of the *Regio* VII and in the Villa di Diomede (http://villadiomede.huma-num.fr accessed on 15 April 2022), has produced an innovative and well-defined methodology for investigating the ancient building in order to identify reparations or reconstruction. It is this particular type of evidence that allow us to recognize traces of damage that are possibly linked to an earthquake (Figure 2).

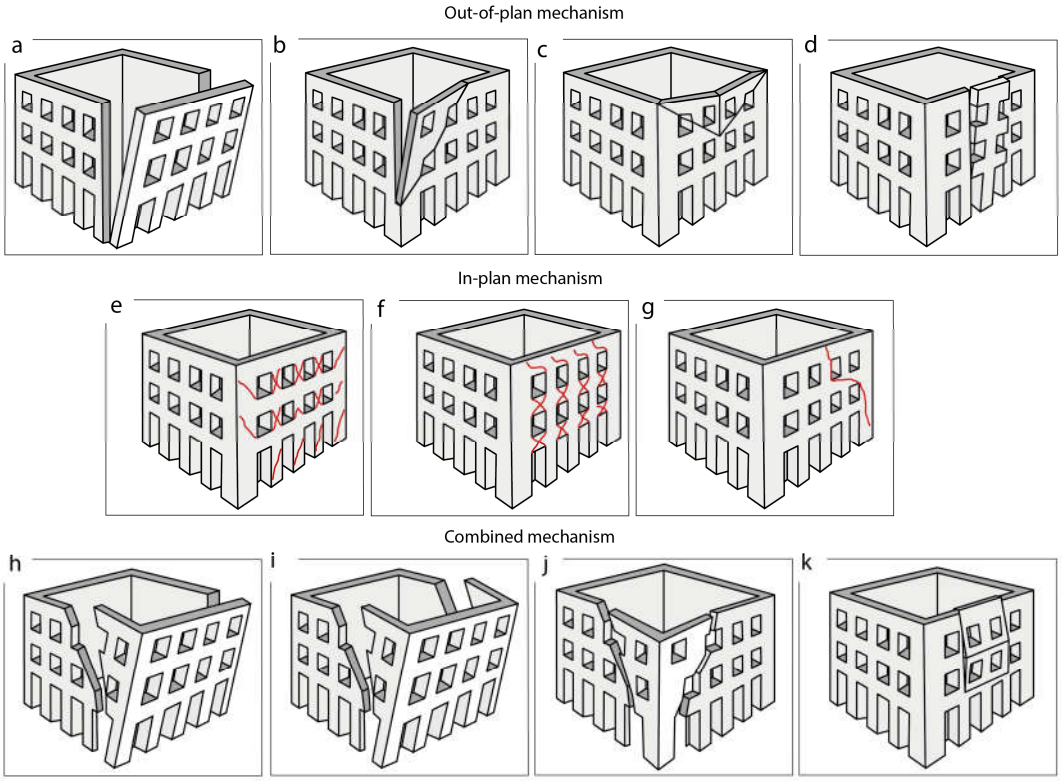

Figure 2. Schematic diagram of possible dissections in relation to a structure affected by a seismic event. Out-of-plane mechanisms: (**a**) total simple overturning of the wall; (**b**) partial simple overturning of the wall; (**c**) horizontal wall deflection; (**d**) offset of the wall. In-plane mechanisms: (**e**) bi-directional injuries at jambs; (**f**) bi-directional injuries in correspondence at sills and lintels; (**g**) one-way diagonal injuries. Combined mechanisms: (**h**) partial complex overturning; (**i**) total complex overturning; (**j**) rollover of the corner of the building; (**k**) vertical wall deflection [37].

More details were provided by a new methodological approach based on the recognition of the Neapolitan Yellow Tuff (NYT) as lithological material used for buildings and also for repairs in the Pompeii urban area [50]. In particular, this study takes into account structural elements containing the NYT lithotypes spread all around the ancient city. The

research led to identify a lot of contexts linked to interventions in the post-seismic period (45 out of 86 studied contexts), demonstrating that the use of this lithotype particularly increased after the well-known 62–63 AD earthquake. From a methodological point of view, the research is based on the study of each individual structural element, which has, as already mentioned, elements in NYT. These elements are identified according to their construction techniques and their static-constructive aspects. First, within the buildings to which they belong, and then, in a more general reading, at the level of each *insula* (block) and each *Regio* (district). This leads to a general reading of the phenomenon of the spread and use of this material, also analyzing the problems directly linked to the earthquakes that struck Pompeii. The study was carried out using three databases and a related GIS. The study of construction techniques was done with the help of the international database ACoR (https://acor.huma-num.fr/ accessed on 15 April 2022) and the analysis of repairs or reconstructions was carried out with the OPUR database (OPUR database downloadable at http://recap.huma-num.fr accessed on 15 April 2022). For the study strictly related to the NYT, a special database, which communicates closely with the other two databases, was created using the FileMaker Pro program [50]. The database entries are based on the cataloguing system adopted by the Pompeii Archaeological Park, enhanced with specific information on the nature of the building materials, the statics of the structures and the wall coverings present, entries related to the conservation of the structures and elements, and the identification of damage, repair, or reconstruction.

All the data collected in the databases were then correlated to the vector plan of the evidence within a GIS, created with the open-source program QGIS. By using this approach, a GIS-based map of the structural elements potentially damaged or restored during or after the earthquake was elaborated [50]. The level of detail in identifying earthquake-related repairs and reconstructions has been raised from the particular to the general. In other words, from the study of each piece of structural evidence, considerations were made at the level of the buildings (some examples can be found in Section 5), which were then used to arrive, in the present paper, at a more general discourse on the individual insulae.

Finally, all the available previous bibliographical data and new recognized data allow us to elaborate a GIS-based map of the damage and restorations of the sectors of the ancient town presenting more site effects due to the earthquakes that preceded its burial in the 79 AD.

2.4. Seismic Homogeneous Microzonation (SHM Map)

The collected data allowed us to identify homogeneous zones roughly characterized by similar geomorphological, litho-, and seismo-stratigraphical features. The merging of available data, managed in the Geographic Information System (GIS), allows us to divide the Pompeii archaeological area into homogeneous parcels of land, each of which characterized by similar stratigraphical, geomorphological, and geophysical features, and to draw the SHM.

In addition, data from the strongest known earthquake (62–63 AD), derived from the DRM map, were used to improve the database on the sectors of the ancient city where site-effects and local seismic amplifications were stronger.

Finally, the work suggests several sectors of the ancient town where further investigations are needed at the second and third levels of SM.

3. Previous Knowledges

3.1. Geomorphological and Geological Setting

The Pompeii ruins are located in the central-northern sector of the Sarno River alluvial coastal plain, close to the southern downslope of the Vesuvio volcano (Figure 3).

The geology of the study area consists of a complex sedimentary history, in which a key role was played by the interaction of several processes such as volcanism, volcano-

tectonic, sea-level changes, and climatic variations, as well as anthropogenic changes. These processes enhanced the strong changes in landforms and environments as well as conditioned the population distribution and settlement strategies; the rise and development of the urbanization, land use changes, economic, and social history; and for Pompeii also its disappearance and preservation, thanks to the burying caused by pyroclastic fall-out and pyroclastic density currents of the 79 AD Vesuvian eruption.

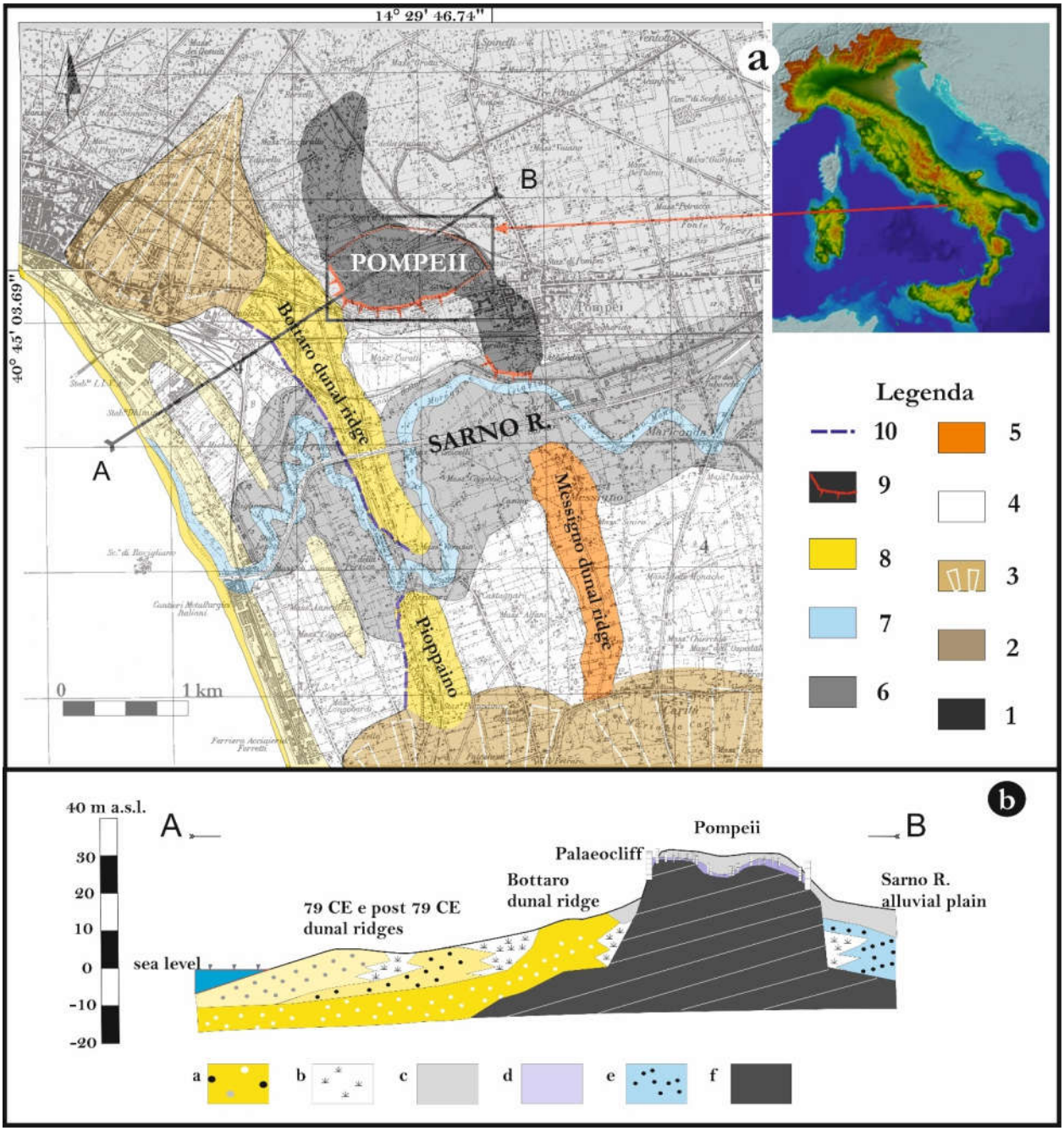

Figure 3. Geology of the Pompeii area. (**a**) Geological map (1:25,000 in scale) of the Sarno river alluvial coastal plain. (1) Pompeii Volcano Lava (late Pleistocene); (2) late Holocene volcaniclastic deposits; (3) late Holocene alluvial fan deposits; (4) Holocene lagoonal, marshy deposits; (5) Holocene dunal deposits; (6) Holocene fluvial deposits; (7) 1800 AD Sarno river paleocourse; (8) Nowadays beach deposits; (9) Early Holocene Pompei paleocliff; (10) 79 AD paleoshoreline; (**b**) Schematic geological cross-section (trace AB) showing a stratigraphic assessment of the subsoil: (a) sandy coastal

deposits; (b) silty-clay marshy and lagoonal deposits; (c) 79 CE eruption deposits; (d) alternating of paleosols, volcaniclastic deposits, and weathered lava; (e) Sarno river fluvial deposits; (f) Pompeii volcano lava.

The ancient city was built on the relics of an ancient volcanic cone, named Pompei Volcano by Cinque and Irollo [23], interpreted as a coalescence of more craters and volcanic landforms, separated by a volcanic complex of the Somma-Vesuvio volcano. The period of activity of the Pompeii Volcano is constrained to the Late Pleistocene and more precisely to the interval that occurred between 40 ka and 20 ka [23,53]. In the urban area, several volcanic landforms were recognized by Cinque and Irollo [23] and they are illustrated in detail in the geomorphological map in Section 4.1.

On the Tyrrhenian sea front, the Pompeii Volcano flanks were cut by seawaves of the transgressive phase of the Early Holocene sea-level rise. A steep cliff, as high as 15 m, was modelled on the western and southern flanks of the volcanic hill. After the transgressive phase, the Pompeii hill and the alluvial coastal plain were under the control of different morphogenetic and sedimentary processes. The hill was mainly formed by erosion or local sedimentation due to gravitational, fluvio-gravitational, alluvial-colluvial and pedogenetic processes. Several volcanic fallouts of the late Pleistocene–Holocene eruptions of the Somma-Vesuvio and Phlegrean Field Volcanoes also were deposited and preserved in local successions [54]. The alluvial plain was indeed formed mainly by aggradative sedimentary events, due to the relative sea-level rise, fluvial dynamics, and volcano-tectonics, and volcanism [55].

In detail, the geology of the Late Holocene was strongly controlled by a decrease in the sea-level rise, driving the coastal sector to the new landscape conformation. Coastal environments were made of dunal ridges and backridge depressions that progressively shifted toward the nowadays coastline. The first dunal ridge, dated to ca. 6.0 ka, the Messigno dunal ridge, was recognized several kilometers into the inner part of the plain, while another ridge, with several phases of growth, was dated between ca. 3.8 ka and 79 CE (Bottaro dunal ridge). Other dunal ridges also were formed after 79 AD and especially during the Middle Age. The coastal progadation was also enhanced by volcanic supply of the Late Holocene Vesuvio eruptions or by ground-level movement due to volcano-tectonics.

The greater late Pleistocene–Holocene eruptions from the Somma Vesuvio volcano that reached the Pompeii area were Pomici di Base (ca. 18 ka); Mercato (ca. 9 ka); Avellino (ca. 4 ka); eruptions named AP (between ca. 3.4 ka and 2.3 ka); the 79 AD Pompeii eruption that caused the burying of the Roman city; and other eruptions between the Late Roman age and the last one that occurred in 1944 AD [54]. Some Phlegrean Field volcano eruptions also reached Pompeii: Neapolitan Yellow Tuff (ca. 15 ka), Agnano Pomici Principali (ca. 11 ka), and Agnano Monte Spina (ca. 4.5 ka) [54].

The surficial and subsoil distributions of the main lithofacies [55] are showed in Figure 3b. They have been grouped into the following:

- From dark-grey well-lithified to dark, poor and reddish foam lava very rich in macroscopic leucite and augite phenocrists. They form the bedrock of the Pompei volcanic hill and are ca. 20 m thick.
- Loose volcaniclastic materials, mainly pumices, scoriae, and ash layers and lava flows, of the Vesuvio volcano southern slopes. A large amount of this unit is composed of fallout and piroclastic density current deposits of the 79 AD eruption.
- Loose and poorly cemented volcaniclastic deposits with intercalated polygenic sandy and gravelly layers of alluvial fan environments, mainly localized in the Lattari mountains and Vesuvio mount footslopes.
- Coastal and alluvial plain deposits composed of dunal and beach sands, lagoonal clays and peats, and sandy and silty fluvial deposits, chronologically constrained to before 79 AD.

- Coastal and alluvial plain deposits composed of dunal and beach sands, lagoonal and marshy clays and peats, and sandy and silty fluvial deposits, chronologically constrained to after 79 AD.

An aquifer is present only in the coastal and alluvial plain deposits at a few meters from the ground level.

As previously described, the ancient city of Pompeii rests on a volcanic hill composed of lava layers and, to the top, by loose and poorly cemented volcaniclastic layers.

The lavic succession is made up by three overlapped lava layers. From the top to the bottom: Unit C (weathered and not-cemented foam lava), Unit B (poorly lithified lava), and Unit A (lithoid lava) (Figure 4). Unit C is composed of foam, scoriaceous, and porous lava layers, from dark to reddish colour, and are very rich in leucite and augite phenocrists, locally named as lava schiuma, spongia, or cruma. The layer, <2 m thick, presents scarce lithotecnical features, being mainly weathered and fractured.

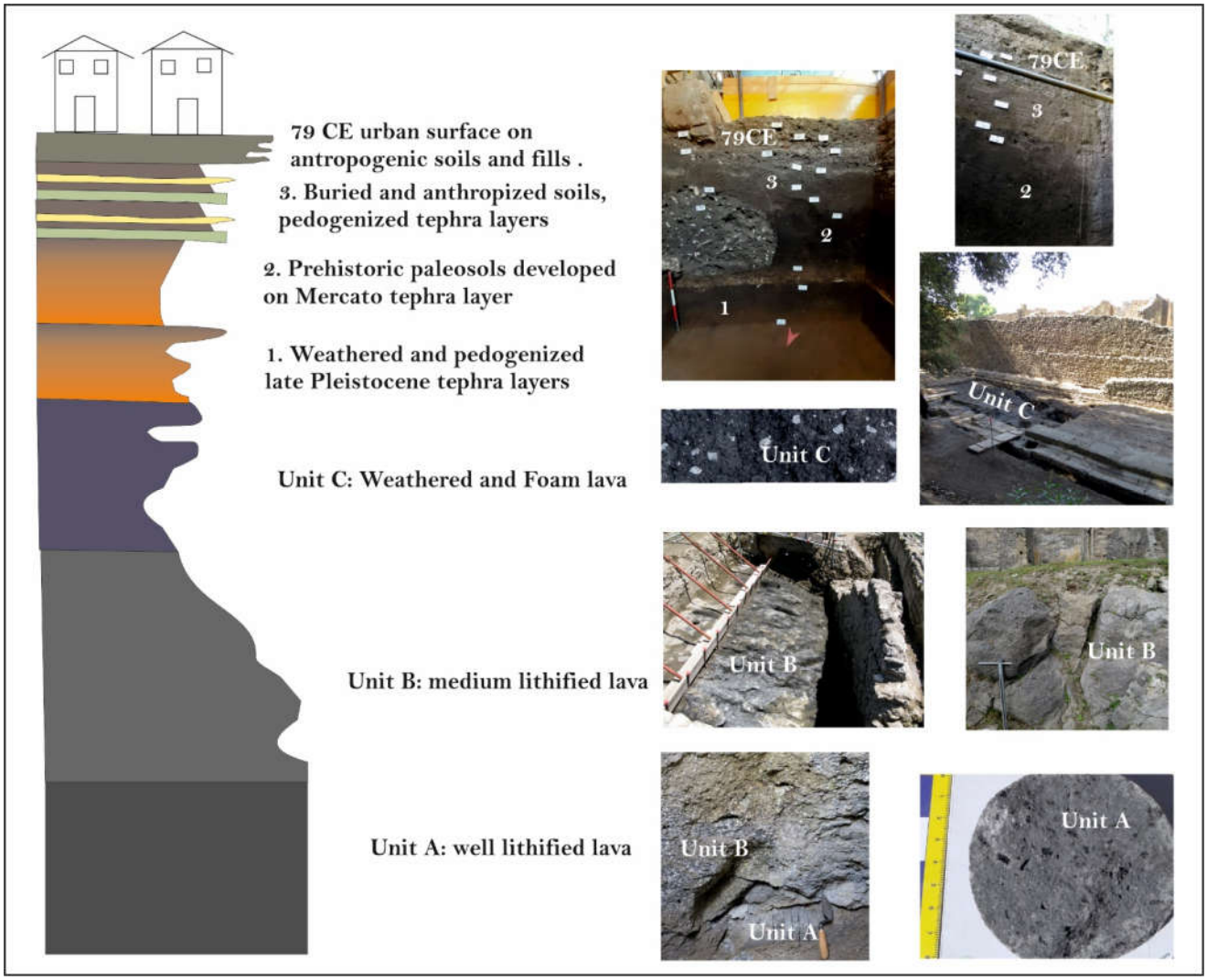

Figure 4. Schematic of the lithofacies log and related photos of the Pompeii subsoil units.

Unit A consists of well-lithified lava, from a dark grey to grey colour, with porphyric assemblage of leucite, augite, sanidine and biotite phenocrists. The rock can be defined as basaltic trachyte-andesite [56,57]. The lithotecnical feature of the lava is good and the thickness also exceeds 15 m. Unit B, 2–3 m thick, presents intermediated features between

the previous ones. Several outcrops of the lava successions are visible in the southern and western slopes of the volcanic hill where the Insulae meridionalis and occidentalis of the ancient city are found. The scarps are the relics of the ancient paleocliff successively modelled by several anthropogenic changes due to quarrying of lava blocks.

On the top of the lava layers, a thin discontinuous succession of pyroclastic layers, paleosols, and anthropogenic fills is presents. An alternating of loose and not-well-lithified fall deposits (mainly millimetric pumices and ashes), dark brown volcaniclastic paleosols, and scarcely sorted coarse anthropogenic deposits, of variable thickness from absent to over 5 m, forms the upper part of the city subsoil. Greater thicknesses are present along the southern and western borders of the city, where the deposits mainly constitute anthropogenic fills, and in local depressions on the top of the volcanic hill.

In detail, the succession to the top of the lava bedrock is composed, from the bottom to the top, of [54]:

- Prehistorical paleosols: made of two horizons: basal, yellow-brown silty sands with intercalations of fine ashes and millimetric pumices of the Vesuvian Mercato eruption (ca. 9.0 ka BP); and upper, dark-brown silty sands very rich in organic materials and bitoturbations.
- Protohistorical and historical paleosols: made of alternating fine ashes and pumices of the Vesuvian eruptions of Pomici di Avellino (3.9 ka) and AP tephra layers (AP2 and AP3 eruptions dated between 3.4 ka and 2.8 ka) and grey-brown paleosols.
- Alluvial and colluvial deposits: made of alternating, loose volcaniclastic silty sands and sandy gravel layers constrained to between the AP tephra layers and 79 AD tephra [58].
- Anthropogenic fills: made of buried and anthropogenic soils, poorly sorted coarse and medium anthropogenic fills, and mainly located within local depressions and along the W and S borders of the ancient city.

3.2. Archaeological and Historical Data on the 62–63 AD Earthquake Effects in Pompeii

One of the major (high in magnitude) earthquakes that affected the ancient city of Pompeii before its burial by the eruption of 79 AD is undoubtedly the earthquake (or seismic sequence) that occurred in 62–63 AD. The earthquake of 62–63 AD has always been the subject of debate among Pompeii specialists, first of all with regard to its dating and then to its actual effects on the city. Even the ancient sources reporting the earthquake do not agree on the time of the event: Seneca in his *Naturales Quaestiones* (VI, 1, 1,2) gives 63 AD as the year of the earthquake, while Tacitus in his *Annales* (XV, 22–23) gives 5 February 62 AD as the date of such an event. Very often double dating has been adopted, such as that proposed in this paper (for recent research on dating to AD 63, see [59]). The seismic event of 62–63 AD, however, was not the only one to precede the dramatic eruption of 79 AD, and in recent decades there have been increasing indications of at least a second large earthquake that can be dated around 70 AD [34,38–51].

On the effects that the earthquake had on Pompeii and its structures, direct evidence of damage is scarce, and few studies have so far attempted to identify the intensity of the earthquake.

The only direct sources are the inscription regarding the reconstruction of the Temple of Isis (VIII 7,28) (CIL X 846) and the reliefs of the *lararium* of the House of *Caecilius Jucundus* (V 1,26), which show the effects of the earthquake in the area of the *castellum aquae* and *Porta Vesuvio* in the relief that has now disappeared (a cast is kept at the Museum of Roman Civilization, inv. 1368) and the second panel depicting the damage caused in the northern part of the Forum (*Parco Archeologico di Pompei*, inv. 20,470) (Figure 5).

Thanks to these first testimonies and to a preliminary reading of the damage to the buildings, in Adam [38] it was estimated that the city had been hit by an earthquake of the IX degree of the MCS scale (also reported by INGV at http://storing.ingv.it/cfti/cfti5/quake.php?50039IT accessed on 20 July 2020, and more recently by

RECAP project [51]). Other specialist studies set the magnitude of the 62–63 AD earthquake at 5.0 [60,61] or 5.8 [62,63].

The urban buildings bear the signs of the earthquake of 62–63 AD and that of the other seisms that have followed and that have certainly had repercussions for Pompeii in political, urban planning, and building terms. In fact, the city did not remain immobile after the earthquakes, but underwent systematic reconstruction in both public and private buildings. There was abandonment, especially in the south-eastern part of the city, and a strong tendency towards speculation, with the purchase of several properties by the same person, a freedman in many cases, and the consequent transformation of houses, often into areas for artisanal use. As far as can be seen, reconstruction did not have a univocal and defined thrust, characterizing itself instead as something chaotic and at times disregarding the rules. The city still had many construction sites active at the time of Vesuvius' eruption, a sign that the area had been extensively damaged and continued to be hit by seismic tremors that damaged even newly rebuilt structures [50,51].

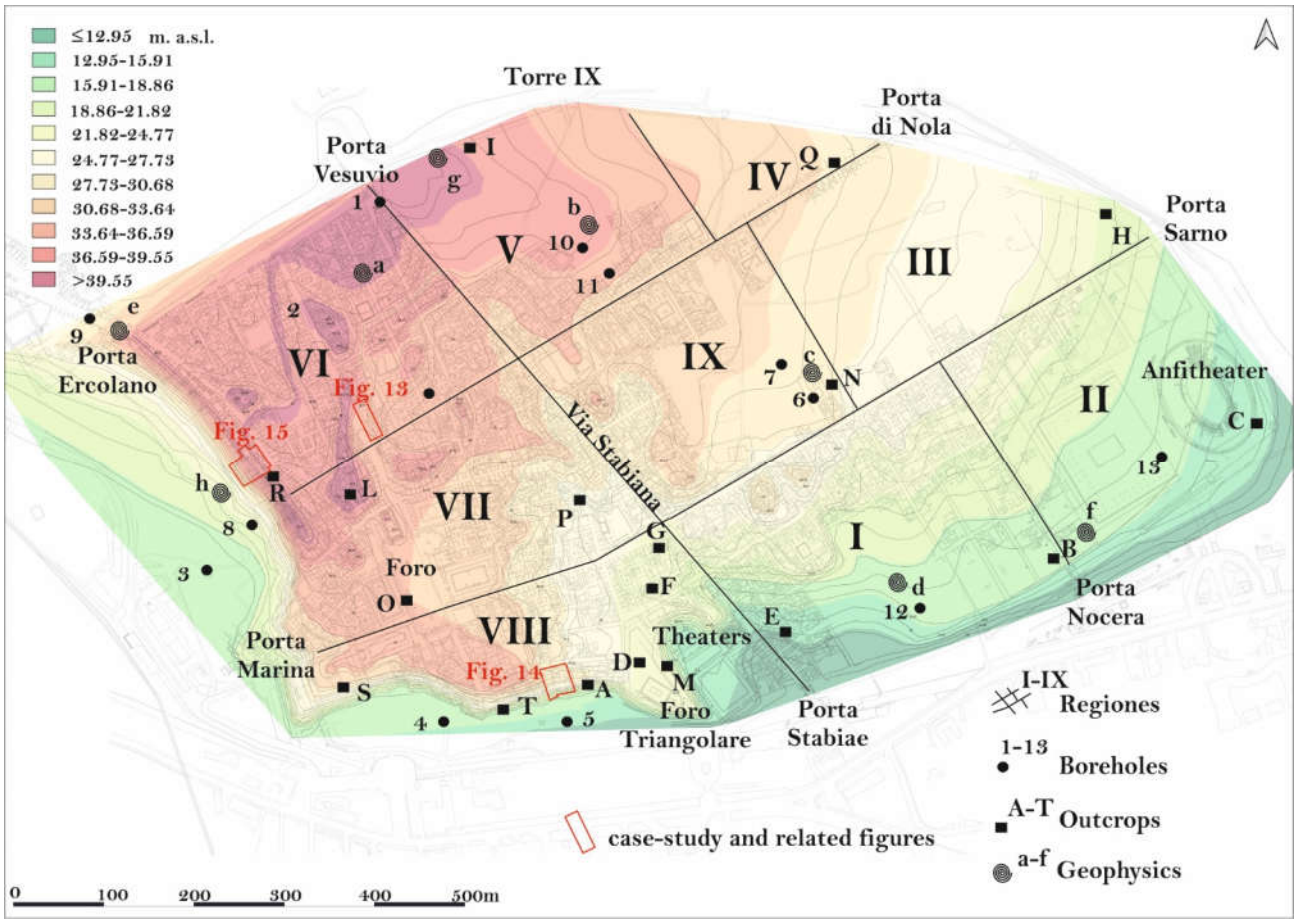

Figure 5. Digital terrain model (DTM) of the Pompeii archaeological area with location of the available data (boreholes, outcrops and geophysical surveys). Also, locations of the case-studies highlighted in the Discussion section are showed.

4. Results

4.1. Geomorphological and Topographical Factors

The urban area of Pompeii is between 42.5 m. a.s.l., in the north-western sector (*Regiones* VI and V), and 15 m. a.s.l., in the eastern (*Regio* II-Amphiteather) and southern (Theaters and *Porta Stabia*) sectors (Figure 6). The geomorphological reconstruction highlights a different topographic setting between the western and eastern sectors, marked by

different landforms and landscapes. They are topographically separated by an ancient concave landform, coinciding with the *Porta Stabia–Porta Vesuvio* road axis. It can be interpreted as an ancient stream landform successively anthropogenically rectified. A great part of the water run off of the Eastern sector and all that of the Western sector flows within it. The impluvium drained (also nowadays) the water of the city toward *Porta Stabia* and, then, toward the Bottaro backdunal depressed sector [55].

The western and southern sectors of the city were built very close to the urban wall circuit, in several cases overlapping and englobing it. They rest on the rim of the ancient palaeocliff, which in these sectors are significantly higher (also >10 m) and present steep slopes (from ca. 90° to 75°), also weathered by collapse and overturning landslides (Figure 6). For this reason, the area of the paleocliff is considered as an unstable zone, firstly for geomorphological factors and secondly for lithotecnical factors (including more thick anthropogenic succession on the top of the lava bedrock).

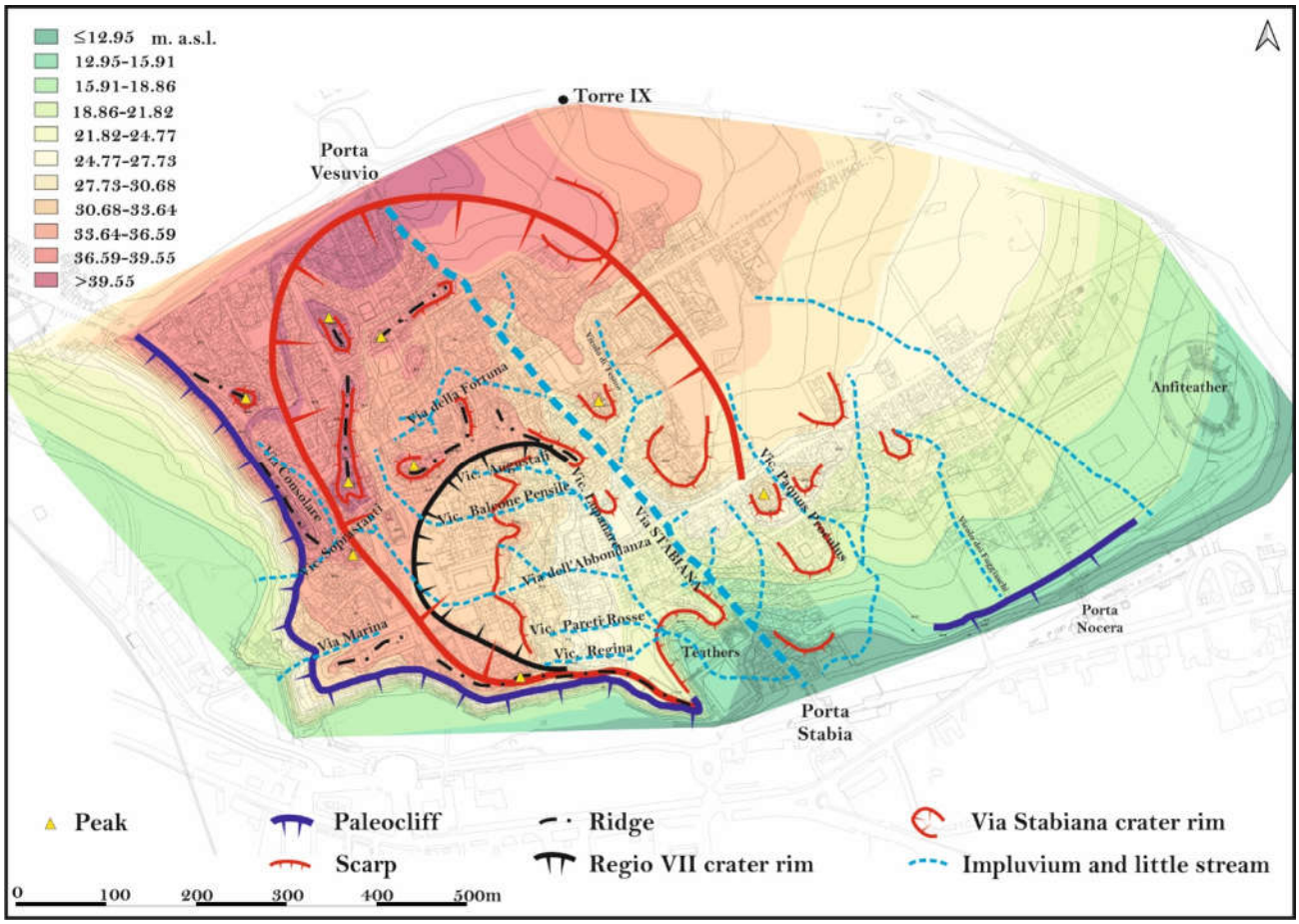

Figure 6. Geomorphological map of the Pompeii ancient city overlayed onto digital terrain model (DTM).

In the eastern sector, the scarp of the paleocliff is lower than the western and southern sectors, presenting also fewer steep slopes.

The western sector of the ancient Pompeii urban area shows very articulated landforms, characterized by several small hills, some of which form narrow and elongated ridges, isolated peaks, and a plateau of reduced extension, edged by scarps and gentle slopes, generally <3 m high [64]. A complex hydrographic network is present between the small hills. It is likely the relic of a more ancient impluvium.

The western and north-western water drainage was guaranteed by several little impluvia (*vicolo degli Augustali, vicolo del Balcone Pensile,* via *della Abbondanza, vicolo delle Pareti Rosse e vicolo della Regina,* in Figure 6), mainly W-E and N-S oriented. They seem to flow firstly into a larger impluvium (*Via del Lupanare* and via *dei Teatri* in Figure 6), ca. N-S and NW-SE oriented, and then into the Theaters area and Via *Stabiana* impluvium. The traces of two other little impluvia (*vicolo dei Soprastanti* and via *Marina* in Figure 6) can be hypothesized to be in the western sector of the ancient city. These impluvia were filled by anthropogenic deposits or changed in underground channels or fully modified. Several archaeostratigraphical data show very thick successions of loose and heterogeneous anthropogenic deposits in correspondence to the impluvia. For these reasons, in this work, the traces of the ancient hydrographical network have been considered as areas prone to local seismic amplification, both for geomorphological and litho-technical factors.

A semicircular landform can be hypothesized between the *Regiones* VII and VIII, likely a relic of a volcanic landform, probably a further crater rim inside the via *Stabiana* crater (Figure 6). The little crater rim can be localized between the *vicolo del Lupanare* and *vicolo degli Augustali* in the N and N-NE sectors and the *Foro* area in the W sector, and between via *delle Scuole* and via *della Regina* in the S sector. In this last sector, the rim merges with the inner part of the via *Stabiana* crater rim, forming a narrow and W-E elongated ridge in the *Foro Triangolare* and *Tempio Dorico* area. The semicircular shape delimits an inside area with higher slopes and scarps, especially localized in the *vicolo di Eumachia* and *vicolo dei Dodici Dei*. These areas also are considered as prone to local seismic amplification.

The sector located to the east of the Via *Stabiana* presents less articulated landforms, marked by gentle slopes, without significative scarps, and planar surfaces gently degrading toward SE. Only the western flanks of the eastern sector present slopes slightly steeper. They can be due to the presence of the eastern inner crater rim of via *Stabiana* and, also, to the large impluvium of via *Stabiana*. A less articulated hydrographic network is traceable for this sector. It seems to flow from NW to SE, in the *Porta Nocera* and Amphiteather area, and from E to W in the via *Stabiana* impluvium. The inner slope of the via *Stabiana* crater and the ancient impluvium are considered as areas prone to local seismic amplification for geomorphological and lithotechnical factors.

Geomorphological Zonation

The geomorphological study allowed us to divide the Pompeii area int homogeneous zone (GM in Figure 7) characterized by three classes of stability/instability.

A. Unstable zones are considered to be those areas presenting scarps higher than 5 m. *Insulae Occidentalis* and *Meridionalis* paleocliff and Theatres areas are included in this category.
B. Stable zones prone to local amplification are considered to be those areas presenting scarps lower than 5 m. There are high gradient slopes (>15°), isolated peaks, ridges, and ancient impluvia, all infilled by anthropogenic deposits and used as underground channels, and are considered to be prone to local amplification.
C. Stable zones are considered to be those showing low gradient surfaces, several meters from unstable areas and all those areas not yet excavated. With regard to those ones, we assume that there are ca. 5 m of 79 AD piroclastic deposits and more recent soils, which have made these areas stable.

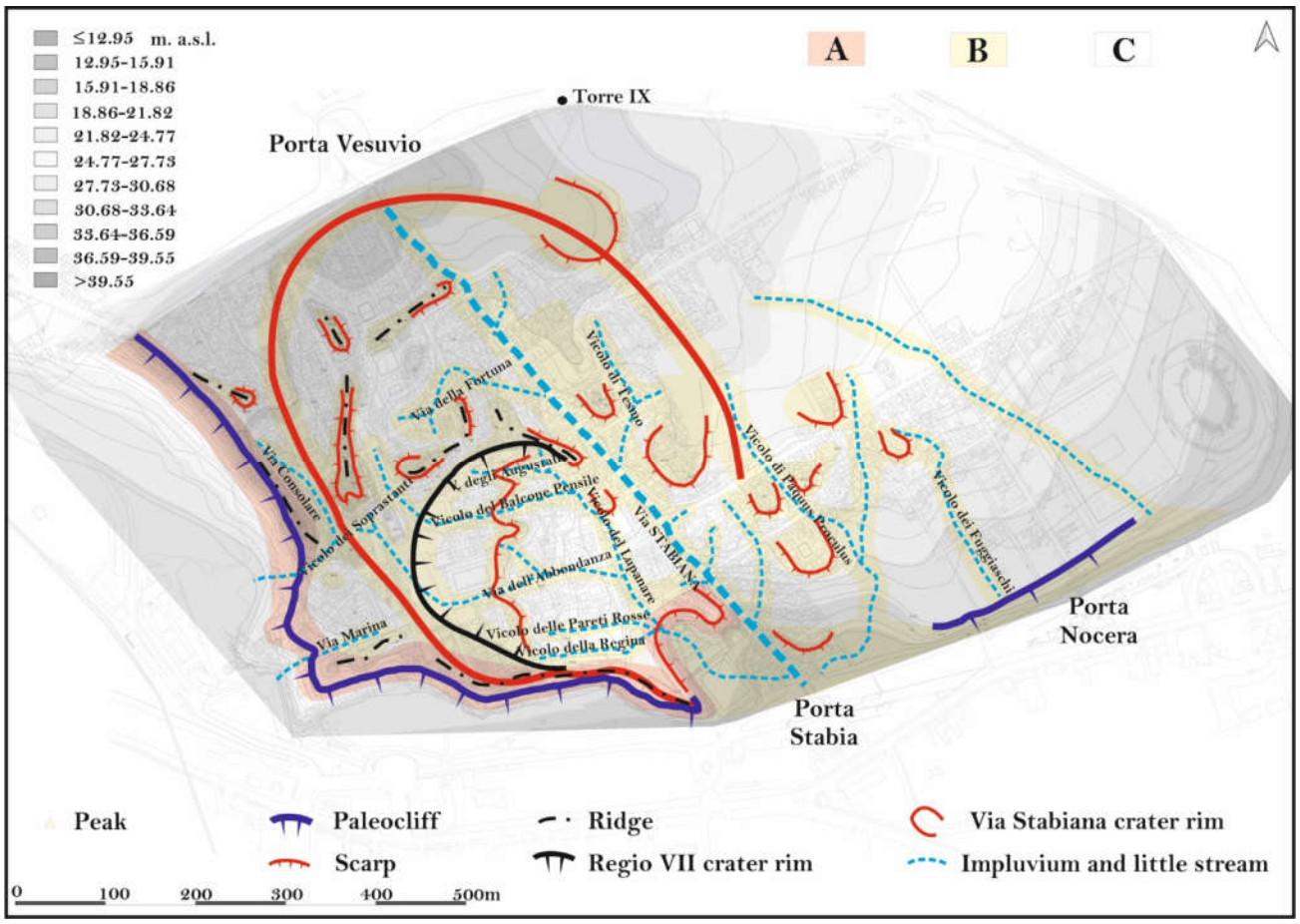

Figure 7. Geomorphological zonation (GM): (A) unstable zones; (B) stable zones prone to local amplification; (C) stable zones.

4.2. Subsoil Data and Stratigraphical Reconstruction

The subsoil of excavated areas of Pompeii Archaeological Park is classified in terms of cover terrain (CT) and bedrock (B). CT are those areas presenting different thicknesses of soft sediments over the bedrock. Buried soils, tephra layers, anthropogenic fills, and unit C of the lava hill are included in this category. The stratigraphical investigation by available boreholes and outcrops (Tables 1 and 2) allowed us to divide the subsoil into four classes (Figure 8): (1) areas without data; (2) areas with a CT thickness less than 2 m; (3) areas with a CT thickness between 2 and 4 m; (4) areas with a CT thickness higher than 4 m. Unit B and C of the lava hill are considered bedrock.

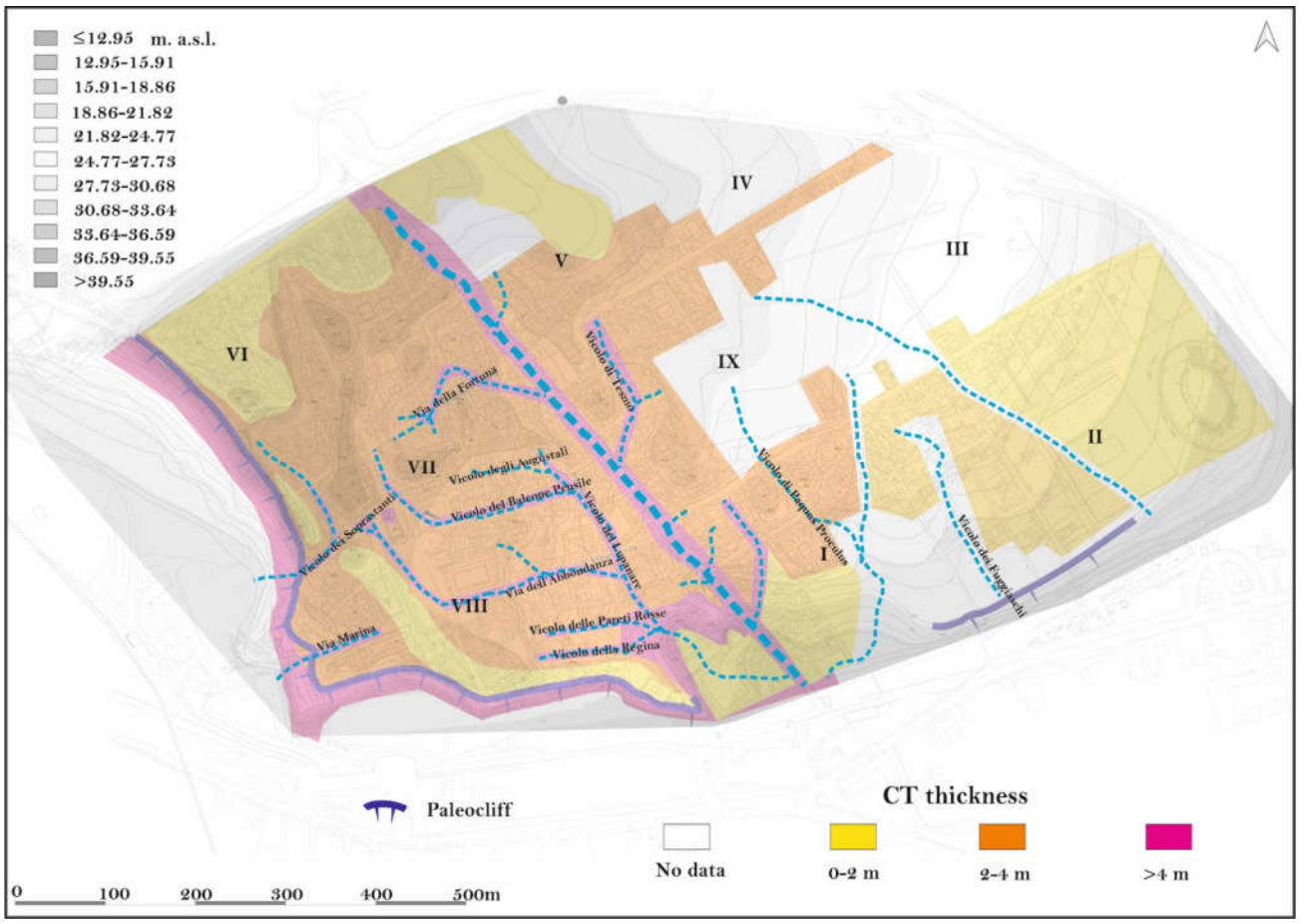

Figure 8. Geological zonation (SGM) and CT thickness distribution. The *Regiones* (I–IX) are showed.

Table 1. Stratigraphical data from boreholes with indication of the CT thickness and B depth from the 79 AD ground level.

Borehole Data				
Code	**Site**	**h (m. a.s.l.)**	**CT (m Thick)**	**B (m Depth)**
1	Porta Vesuvio	41	3.1	3.5
2	*Regio VI Insula 13*	38	13	13
3	*Insula occidentalis*	35	15	>15
4	*Insula meridionalis*	25	4	5
5	*Insula meridionalis*	25	5	5.5
6	Casti Amanti	27.5	3.5	4
7	Casti Amanti	28.5	3.5	4
8	*Insula occidentalis*	10	1	2.5
9	Villa dei Misteri	40	2	2.5
10	*Regio V*	37	4	4.5
11	*Regio V*	35	5	5.5
12	*Regio I*	13	0.5	0.5
13	Palestra grande	14	0	1
a	Vicolo dei *Vettii*	36	3	3.5
f	Porta Nocera	15	3	3.5

Table 2. Stratigraphical data from outcrops and archaeological excavations with indication of the CT thickness and B depth from the 79 AD ground level.

Outcrop and Archaeological Trench Data				
Code	**Site**	**h (m. a.s.l.)**	**CT Thickness (m)**	**B Depth (m)**
A	*Insula meridionalis*	25	0	1
B	Porta Nocera	16.5	1	1.5
C	Anfiteatro	15	0	0
D	Foro triangolare	24	0	0.5
E	*Regio I*	14	0.5	0.5
F	Casa di Giuseppe II	23	3	3.5
G	Casa dei *Postumii*	24	3	3.5
H	Porta Sarno	23	0	1
I	*Regio V*	40	4	4.5
L	*Regio VII*	40	1	2
M	Foro Triangolare cisterne	23	>10	>10
N	Casti Amanti	28	3.5	4
O	*Forum*	34	1	2
P	Vicolo del Lupanare	27	5	5.5
Q	Porta Nola	30	1	2
R	Via Consolare	38	1.5	2
S	Tempio di Venere	32	3	3.5
T	*Insula meridionalis*	24	3–8	5

The first class includes non-excavated areas.

The second class (<2 m of CT thickness) is mainly concentrated in the NW and N sectors of the ancient city between *Porta Ercolano* and *Torre IX*, in the E sector between *Porta Sarno* and Anfitheater, in the area of *Porta Stabia* and along the ridge of the ancient volcanic rim in the W sector.

The third class includes a large sector of the ancient city, mainly localized in the central part between *Regiones* VII, VIII, IX, and I.

The fourth class includes the sectors of the paleocliff of the *Insulae occidentalis* and *meridionalis* between the ancient city walls and several houses and villas built directly on them. In several cases, the foundations of the buildings rest on thick anthropogenic fills, anciently reported to be on the scarp in order to enlarge the size of the houses. CT thicknesses higher than 4m are present also between the *Foro Triangolare* and Theaters area and in the ancient impluvium paleomorphologies.

4.3. Geophysical Data and Seismo-Stratigraphy

The available geophysical data consist of 4 seismic tomographies (seismic refraction) carried out for *Regiones* IV, V, and I, and in 7 MASW carried out for *Regiones* IV, V, VI, VII, and I (Figure 5). The seismic tomographies allow us to characterize the velocity of the P waves (Vp) in the subsoil of the Pompei Archeological Park until to ca. 30 m of depth. The MASW analyses allow us to characterize also the S wave velocity (Vs) and to evaluate the Vs30.

In detail, the seismic tomographies show three main seismo-layers (Table 3):

A. From the ground level to ca. 2–5 m of depth, a layer with values of Vp less than 300 m/s, linkable to the presence of anthropogenic fills and loose pyroclastic layers and paleosols (CT).
B. From 2–5 m to 7–10 m of depth, a layer with values of Vp between 300 and 600 m/s, linkable to unit C of the lava bedrock.

C. From cca. 10 m to cca. 30 m of depth, a layer with values of Vp higher than 600 m/s and progressively exceeding 1000 m/s in depth, linkable to unit A and B of the lava bedrock.

Starting from these data, it is possible to interpret the A and B seismo-layers as CT and the C seismo-layer as SB.

MASW analyses, relative to the velocity of the Vs in the subsoil of Pompei, also confirm these seismo-stratigraphical features. In detail, the analyses show three main seismo-layers:

A. From the ground level to cca. 5 m of depth, a layer with values between 300 and 500 m/s, linkable to the presence of anthropogenic fills, paleosols, and pre 79 AD pyroclastic layers.
B. From 5 m to cca. 10 m of depth, a layer with Vs values between 500 and 600 m/s, linkable to weathered lava bedrock (Unit C).
C. From ca. 10 m to ca 30 m., a layer with Vs values higher than 600 m/s, linkable to lava bedrock.

The Vs 30 evaluation shows values between 300 and 500 m/s.

Table 3. Geophysical data and seismostratigraphy of the Pompeii subsoil. Characterization of the Vp and Vs wave velocity and evaluation of the Vs30.

Regiones		Layer A		Layer B		Layer C		
		Depth (m)	**V (m/s)**	**Depth (m)**	**V (m/s)**	**Depth (m)**	**V (m/s)**	**Vs30 (m/s)**
***Regio* I**	**Vp**	0–3.5	234–361	3.5–10	467–748	10–30	867–1198	423
	Vs		94–253	3.5–8.9	436–470	8.9–30	605–845	
***Regio* IV**	**Vp**	0–5.5	198–389	5.5–11.2	486–802	11.2–30	899–1219	457
	Vs	0–5.7	94–257	5.7–8.6	317–399	8.6–30	499–808	
***Regio* V**	**Vp**	0–5.1	245–288	5.1–9.9	378–792	9.9–30	852–1344	318
	Vs	0–5.7	107–215	5.7–12.2	271–405	12.2–30	4470–645	
***Regio* VI**	**Vp**	-	-	-	-	-	-	316
	Vs	0–5.5	185–315	5.5–11	340–382	11–30	431–600	
***Regio* VII**	**Vp**	-	-	-	-	-	-	364
	Vs	0–4.6	207–216	4.6–10	265–397	10–30	482–654	
***Regio* VII**	**Vp**	-	-	-	-	-	-	324
	Vs	0–4.7	115–197	4.7–10	284–316	10–30	372–665	
***Regio* IX**	**Vp**	0–3.3	315–412	3.3–9.3	596–807	9.3–30	1134–1394	486
	Vs		149–228	-	421–543	-	602–868	

These data allow us to elaborate the geophysical model of the subsoil of Pompeii and to draw the geological/geophysical map (GGM) that include also lithostratigraphical characterization of the subsoils. In addition, a better evaluation of the CT thicknesses and SB depth was carried out. First of all, total CT thicknesses includes CT + Unit C of lava bedrock and only the lava not showing weathering and fracture can be considered SB. For this reason, the lithostratigraphical distribution of the CT showed in Figure 6 was corrected, adding further thicknesses of the weathered lava (seismo-layer B). The schematic representation of the geological–geophysical model map (GGM) is showed in Figure 9.

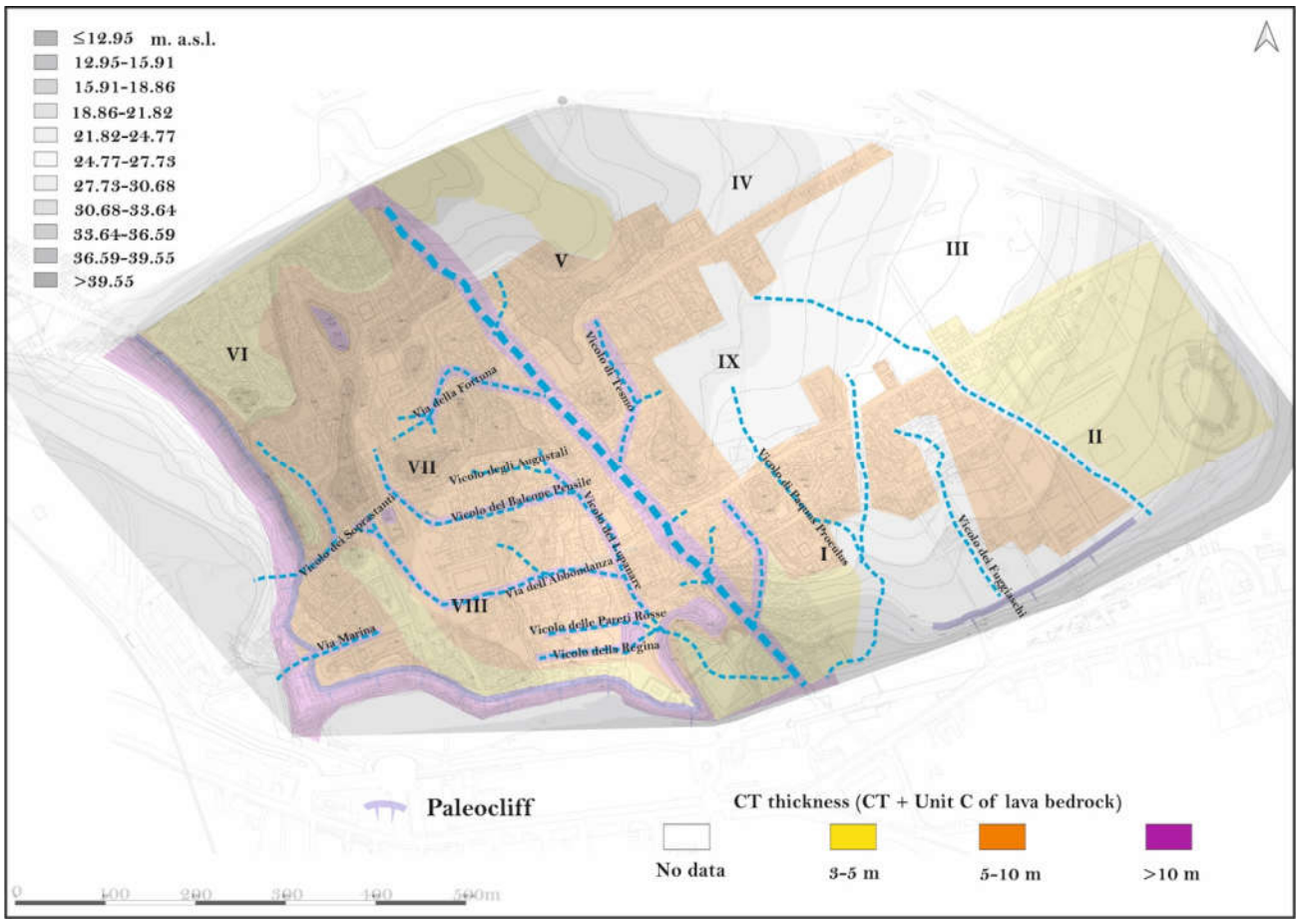

Figure 9. Geological/geophysical model map (GGM) and corrected CT thicknesses (CT + Unit C of the lava bedrock). The *Regiones* (I–IX) are showed.

4.4. Archaeological and Architectural Field Recognition and Distribution of the Main Damage and Reconstruction due to the 62–63 AD Earthquake in Some Selected Buildings

Previous studies ([34,38,40–51], and references therein) concerning the identification of some damage, repairs, and reconstruction, made it possible to produce a first chart mapping the level of damage, repairs, reconstructions, and construction sites still in progress in Pompeii.

As can be seen in Figure 10, the areas in which there is the highest amount of evidence of earthquake-related damage or construction works are in the southern (VIII 2) and western parts of the city (VI 17 and VII 16).

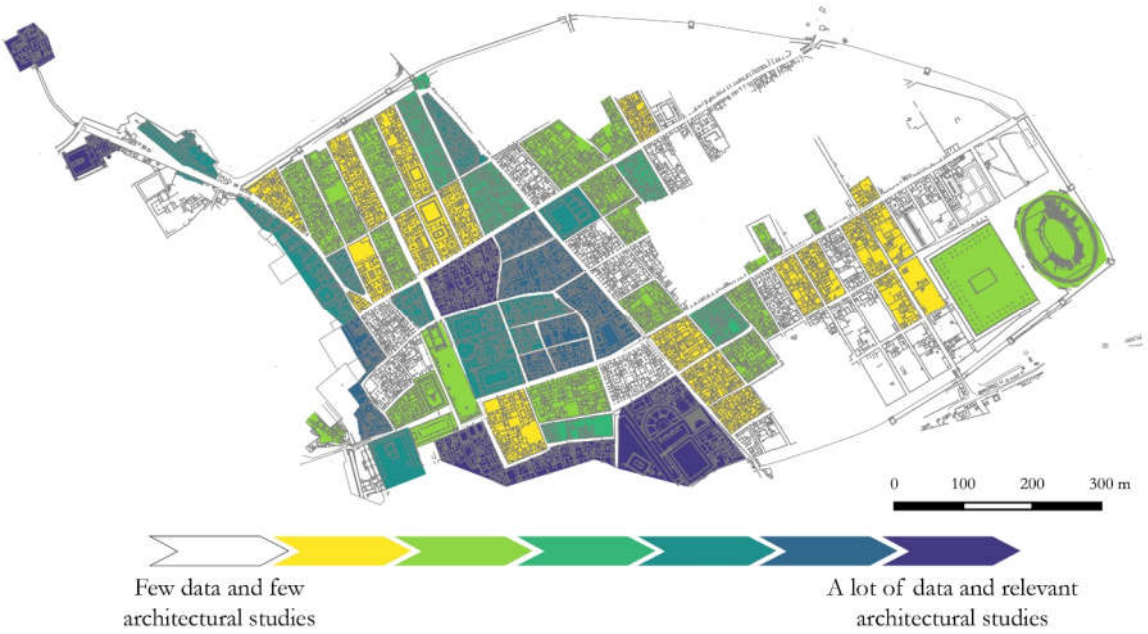

Figure 10. Assessment of damage and post-seismic repairs based on recent scientific literature (elab. M. Covolan); data from [38,40–51,65–81].

Taking also into consideration the data from the study of the structures made of Neapolitan Yellow Tuff, it was possible to investigate the presence of repairs made with this building material all over Pompeii.

The types of interventions most commonly presented and attested are repair of the corner chain (portion in correspondence of the corner formed by two structures, often masonry); creation of a buttress (masonry structure unrelated to the damaged structural element, but with the function of static support to it, which may be either a pillar or a larger structural element); complete reconstruction (the original portion of the structure is preserved only in small points in the same structural element or in those directly connected); reconstruction of the piers of an opening (reconstruction may also involve a portion of the masonry adjacent to the pier, and may therefore present a reconstructed part of the facing in addition to the limit of the opening); and plugging (an operation that may be linked either to a change in the pathways within a building, or from a static point of view, when the intention is to strengthen a structure that risks collapsing in correspondence with the opening that is being obliterated).

The data about the number of repairs made with this material is obviously partial, compared to the total number of repairs and reconstruction in the city. For example, looking at the data from the RECAP study [51], it can be seen that repairs or reconstructions in NYT are a small fraction (only 8,5%) compared to those made of clay elements. This aspect is very important because even if only considering the repairs made with this material, we have an important clue about the trend in the number of repairs for each *Regione*. A high number of elements reconstructed or repaired with the NYT can therefore denote a high degree of reconstruction in those areas and it is on this assumption that the following discussion is based. If we refer to the graph regarding the distribution of reconstructions at the *Regiones* level (Figure 11), we can clearly see that these interventions are more concentrated in *Regiones* VII, VI, and VIII, with respectively 40, 31, and 16 attestations, thus covering 89.6% of all cases identified in the research. Particularly, in *Regiones* VI and VII, it can be seen that all the types of repairs mentioned above are widespread.

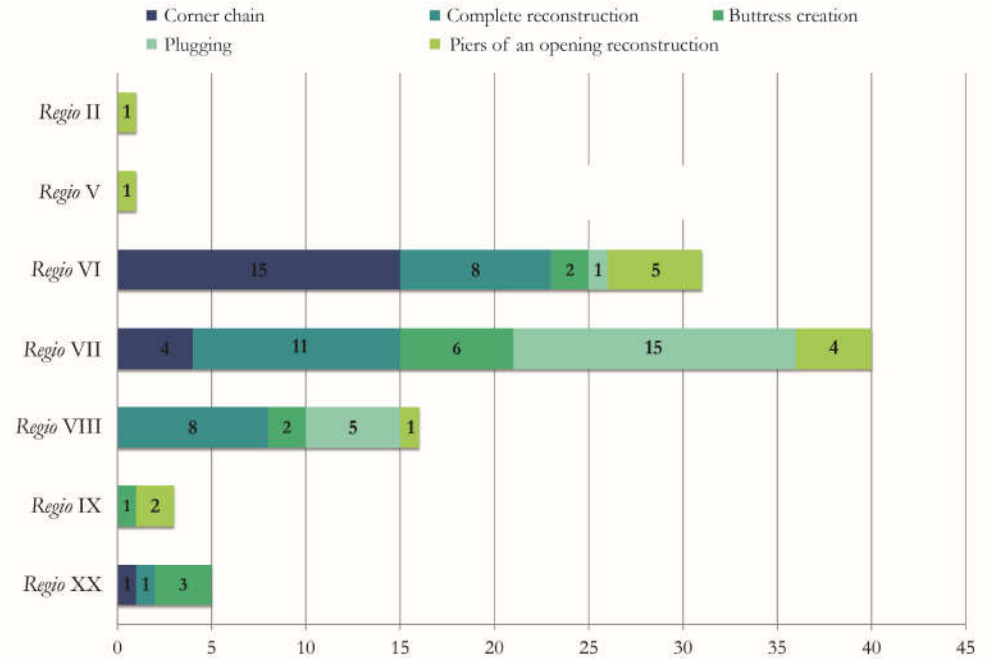

Figure 11. Graph of the distribution of the various types of repairs realized in NYT within the different *Regiones* [50].

From these data and the fact that *Regiones* VI and VII also have the highest number of NYT structural elements, especially those that can be dated to the post-seismic period, some interesting questions emerged, which we decided to investigate more specifically.

The possibility of cross-referencing geomorphological and archaeological data was thus considered in order to produce a first version of a seismic microzonation map of the territory of the ancient city of Pompeii, with the aim of defining predisposing and causative factors for the assessment of vulnerability and seismic hazard.

As can be seen from the intersection of the geomorphological map with the volume of contexts in which the NYT is used, it is clear that some buildings, which also have a fairly high number of structures in NYT, are located in areas that can be considered as unstable zones or stable zones prone to local amplification. Other buildings are located in points where, from the topographical point of view, there is the presence of pre-existing underground structures, in conjunction with anthropogenic deposits (soft-sediment), for example, along the circuit wall; others are located in points where it is possible to highlight the presence of impluvial lines or topographical contexts capable of amplifying the seismic waves of an earthquake.

Obviously, the first reading that is given here does not take into account characteristics related to construction techniques or materials used, since such a study is very extensive and would require a specific analysis for each individual building, with the intervention of numerous experts from different disciplines. The first conclusion that can be drawn from the crossing of data is that, if there is a certain number of structural elements within the same context or in neighboring buildings that date back to the post-seismic period and that present NYT within them, we are very likely in a context or area of the city where there has been a lot of damage.

In the following section, we analyze three case studies for which it is particularly evident that the rule of geological and geomorphological site effects connected to damage or restorations due to earthquakes are highlighted with the NYT study.

5. Discussion and Seismic Microzonation of the Pompeii Archaeological Park

Geomorphological, lithostratigraphical, geophysical, and archaeological data merging allow us to identify five classes of seismic homogenous microzones: four SHM stable zones and one SHM unstable zone (Figure 12).

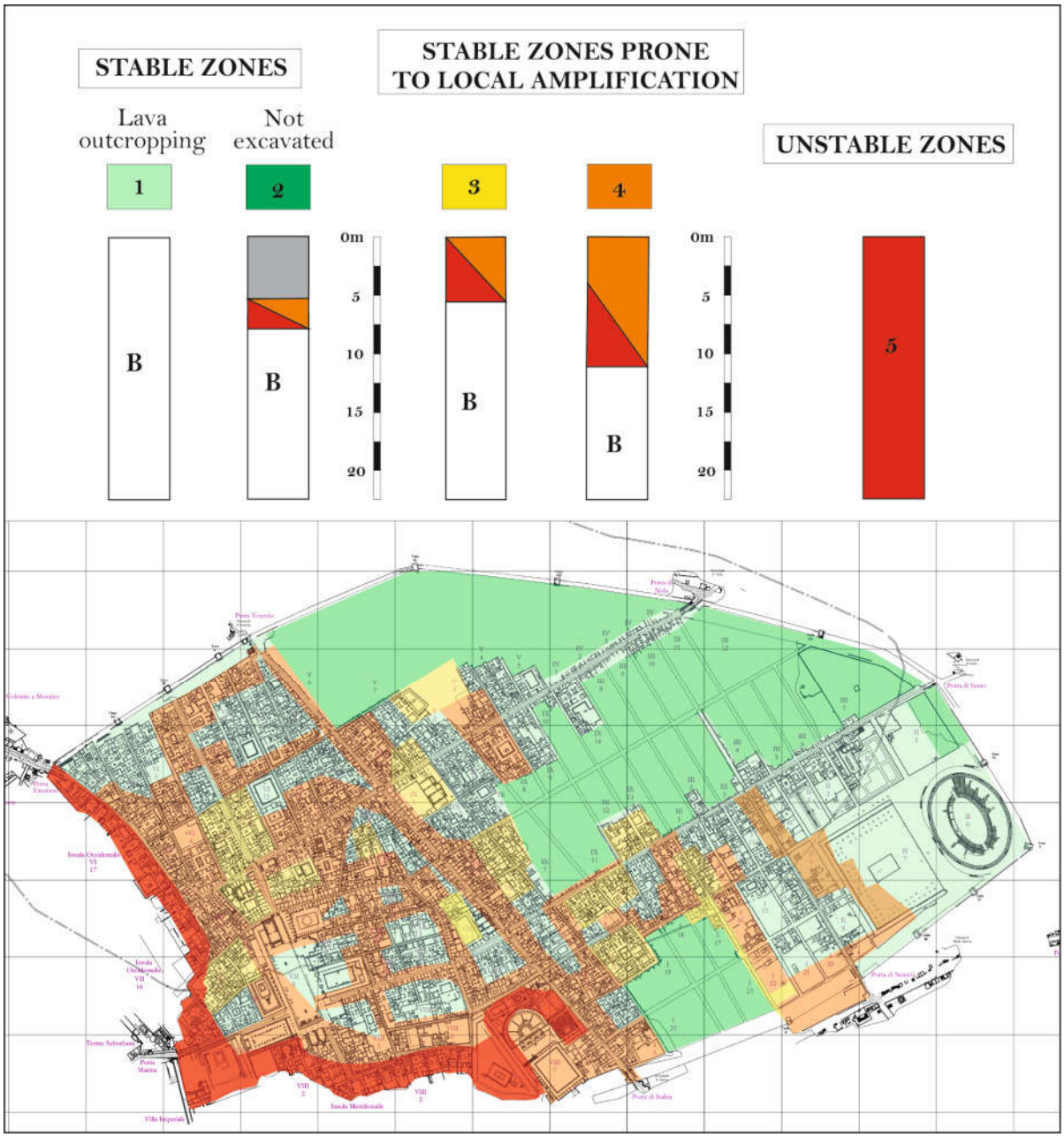

Figure 12. Seismic homogeneous microzones and seismic microzonation map of the Pompeii Archaeological Park.

The stable zone can be divided in two sub-classes: two SHM stable zones and two SHM stable zones prone to local amplification. The stable zones include still unexcavated areas (SHM 1) of the ancient city and areas of lava outcropping without CT and topographical site effects (SHM 2), characterized by values of Vp and Vs higher than 600 m/s and progressively exceeding 1000 m/s in depth.

The stable zones prone to local amplification include areas with CT thickness variable from <5 m (SHM 3) to ca 10 m (SHM 4), also including unit C of the lava bedrock, characterized by values of Vp and Vs between 300 and 600 m/s or lower than 300 m/s. In SMH 4, also topographical site effects are included.

The unstable zone includes areas where greater topographical, lithotecnical and geophysical site-effects are expected.

SHM 1 are mainly localized in the eastern sector of the city (Amphitheater and *Palestra Grande* areas) and secondly in several small-size areas where CT and topographical factors are absent.

SHM 2 is related to still unexcavated areas of the archaeological park, mainly localized in the E and NE sectors. In these sectors, the 79 AD eruptive deposits cover the ancient ground level of the city with ca. 5 m of medium thickness. Being archaeological heritage buried in the subsoils, these unexcavated areas can be considered as stable zones.

SHM 3 are related to little zones showing a CT thickness <5 m and significantly far from local topographical factors.

In these SHMs, a great part of the buildings do not show significant traces of damage or restoration during the post-seismic period (between 62–63 AD and 79 AD), as in the case study of the House of the *Naviglio* (VI 10, 8–9.11; Figure 13) [82–86].

Figure 13. On the left is the plan of House of the *Naviglio* (VI 10, 8–10), with in red the structures built up with NYT elements. On the right the plan of the geomorphological evidence in the same area (elab. M. Covolan).

The house is the result of the union of two buildings, which originated as independent in the first half of the 3rd century BC. One dwelling has remained fairly unchanged over the centuries, the one accessible at No. 11, while the other, which must have been accessible from No. 8, is nowadays not preserved except for the remains of the impluvium of the atrium. The two dwellings were incorporated into one already around the end of the 2nd century BC, creating a garden in the northern part.

In the post-seismic period (between 62–63 AD and 79 AD), some changes were made, with newly formed spaces and perhaps an upper floor, which were previously non-existent, being added. No heavy interventions on the structures can be identified, except for some reinforcements in some of the garden walls. This is the case of the three interventions made in NYT and clay elements. In all three cases, these are reinforcements of corner chains in walls that are not aligned with each other and are therefore weak from a static point of view.

The house is quite far from significant topographical factors and presents a CT thickness <5 m. Likely, it reflects a lesser presence of structures in NYT elements of the post-seismic period, and the limited interventions identified relate to structures that are already weak in themselves.

SMH 4 are mainly localized in correspondence to significant local topographical factors (peaks, little hills, ridges, scarps, underground channels, and ancient impluvium landforms). Furthermore, the sectors showing CT thicknesses >5 m are included in this SMH.

In these SHMs, a great number of buildings shows traces of damage or restoration after the 62–63 AD earthquakes, as in the case study of the House of *Francesco Giuseppe* (VIII 2, 29–30; Figure 14) [87–91].

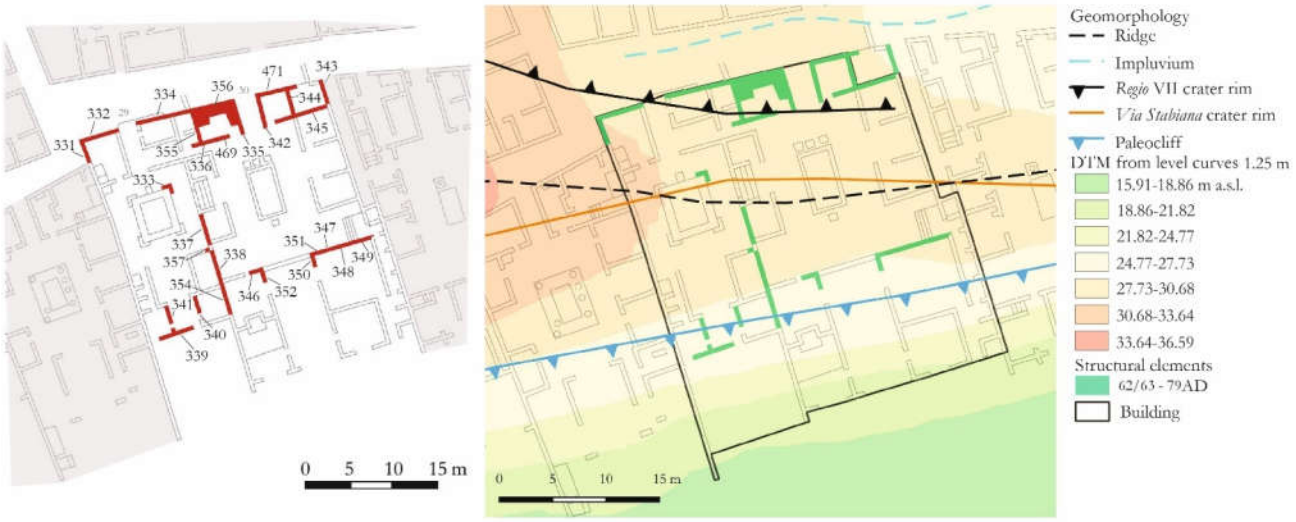

Figure 14. On the left is the plan of House of *Francesco Giuseppe* (VIII 2, 29–30), with in red the structures built up with NYT elements. On the right, the plan of the topographical factors in the same area (elab. M. Covolan).

The original building plan and structures date back to the 2nd century BC and here, originally, there were two separate houses. One of the edifices, accessible from No. 30, was at first developed southwards till the city walls, and has two levels, the ground floor and the below terrace structures. The second house, the one at No. 29, was shorter and its facade was set back with respect to the present walls: the ancient facade had the same orientation of the front part of the nearest west building. In the middle of the 1st century BC the two houses were joint and a lot of modifications were carried out, especially with regards to the rebuilding of the edifice facades. The new big building was characterized by two atria, an underground floor occupying the entire width of the building and a first floor, at least partially over the occidental portion of the house. The house suffered a lot during the 62–63 AD earthquake: lots of damage occurred in all the sectors of the dwelling and these caused a redistribution of the internal paths and the destination of the east part of the house as the representative area. The basement seemed no longer accessible and various walls, especially the ones of the facade, were rebuilt. The restoration works were not concluded in 79 AD: at that time some plastering was still under maintenance or had not been made yet; moreover, there was a basin for mixing mortar still in use in the south-east corner of the western atrium.

In this building, in particular considering the structures presenting elements NYT, it is possible to better analyze what happened after the earthquake. Some of the damaged walls were rebuilt completely (structures No. 331–336, 338, 342–345, 349–352, 354–356, and 471) or partially reconstructed, such as the wall at No. 337. In one particular case (No. 357),

a buttress was realized in order to prevent the collapse of a wall that suffered the seism, but that did not need a complete reconstruction.

There is also a series of interventions (structures built up only with NYT rectangular elements) that allowed us to identify a second phase of the works (structures No. 339–341, 346–348, and 469). If we analyze the position in the plan of some of these new structures (No. 346–348 and 469) and their static function, it is possible to suggest that they might have been the consequence of a second big earthquake, which hit Pompeii between 62–63 AD and the year 79 AD. These last new walls were erected in order to close some doors or passages, which might have been too fragile to resist another seism. In another case (No. 339–341), the interventions seem merely due to a change in the internal paths of these big complex.

Connecting this construction information with the geological and geomorphological settings of the area (Figure 14), it can be immediately noticed that the building is located in an area characterized by the presence of a very steep escarpment, the ancient city walls, and therefore also the related soft-sediment embankments. In terms of slopes, 49.3% of the total area of the building is on a slope greater than 35%; 53.8% of the area is in an area with slopes between 10% and 25% and finally 15.8% of the surface is in areas with a slight slope (<5%).

In addition to this, the house was built on the ridges of the crater rims of Via *Stabiana* and *Regio* VII, and found on non-uniform CT thicknesses, variable from >5 m in the southern and northern parts and <3 m in the central part of the house. In addition, the northern part of the building is also in proximity to the *Vicolo della Regina* impluvium, which was supposed to drain the wastewater towards the east, in the area of the Triangular Forum, starting from the 5th century BC and then filled with anthropogenic sediments. In terms of anthropogenic interventions, we should not forget the rooms built on terraces sloping towards the south and those partly hypogeal, also set in and above the curtain wall and its filling levels.

In the same area, the presence of the abovementioned impluvium may also be the cause of the unevenness, later restored, identified at *Hortus* VIII 6, 2, opposite the house under examination. In this case, too, the damage caused to the structures, which were also rebuilt in NYT (pillars of a big porch and two adjacent walls in the south-east corner of the building), are due to the amplification of the seismic waves due to local topographical factors.

The unstable zones (SMH 5) are localized in correspondence to the ancient paleocliff where several buildings were found on >10 m scarps and, many times, over several meters of anthropogenic deposits. The theatres area and partially *Foro Triangolare* area also were built on several meters of anthropogenic deposits and along a steep slope.

For these SHMs, almost all the buildings show clear traces of damage and restorations after the 62–63 AD earthquake, as in the case study of the House of Diana II (VI 17, 32–36; Figure 15) [92,93].

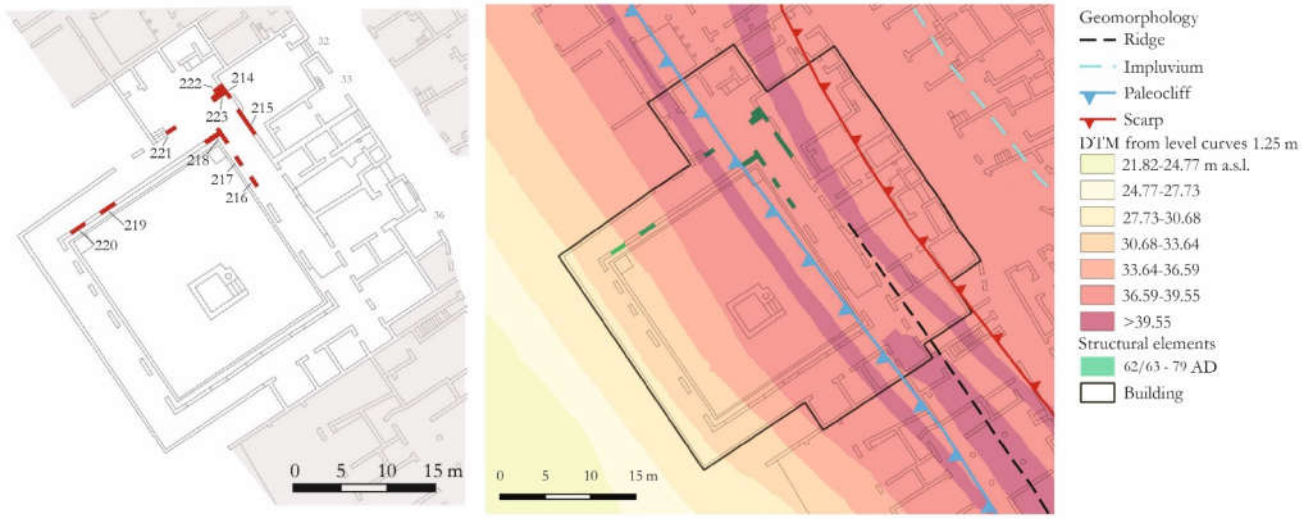

Figure 15. On the left is the plan of House of Diana II (VI 17, 32–36), with in red the structures built up with NYT elements. On the right, the plan of the geomorphological evidences in the same area (elab. M. Covolan).

This ample house presents various levels sloping down towards the West. Not all the floors are accessible today and all of the western side is very compromised. The original plan was organized around two main atria leading to a unique big peristyle. The access from the street was very peculiar and not so common among the houses' entrances in Pompeii: both atria were linked to the street with little stairs. The whole building is developed at a higher walking surface compared to the street and its underground floor is only a sub-basement in the east portion. The peristyle is situated at another higher altitude compared to the atria on an artificial terrace in the middle, of which there used to be a cistern that is no longer visible.

After the 62–63 AD earthquake various interventions were made inside the house to restore the damage caused by this seism and probably the works were not concluded in 79 AD. The structures having NYT elements are the new western walls of the atrium (No. 214 and 215) accessible from No. 32, the adjacent *lararium* in the north-east corner of the peristyle (No. 222 and 223), and the pillars contouring the garden (No. 216–221). The pillars are peculiar, with a semi-column in the middle of the front, realized in masonry. In some cases, the half-column was made with a hidden fictile pipe, which led the rainwater from the roof to a system of canalizations forming to the cistern. The intercolumnio, at least those well-preserved ones, were closed with a wooden frame, probably supporting a window glass. This last architectural solution and all the structural elements in NYT, seem to be a post-seismic intervention.

The House of Diana II is located very close to the escarpment of the ancient paleocliff, but also on a ridge of the crater rim of Via *Stabiana*, above the disused city walls and with a lot of anthropogenic fills related to both the city walls and the levelling of the area for construction on several staggered levels. Other destabilizing elements are also the numerous underground rooms and also the cistern in the center of the peristyle. In terms of slope, 68.3% of the total area is on land with a slope of more than 35%, while 29.9% of the building is almost flat, with a slope of less than 5%. In the vicinity of this building, to the east of the road in front of the house, there is also an ancient trace of the Via *Consolare* impluvium, which is currently buried and filled with soft-sediment.

6. Final Remarks and Conclusions

The multidisciplinary approach used in the present paper allow us to draw, for the first time, the seismic microzonation map (level 1) for the Pompeii Archaeological Park

and to lay the basis for detailed seismic microzonation studies (Levels 2 and 3) for the risk assessment of one of the most important archaeological site in the world.

The study shows how the local topographical factors and non-uniform distribution of CT thicknesses played a key role in the seismic wave amplification during the 62–63 AD earthquake. For these reasons geological and geomorphological factors must be taken in great consideration for planning of mitigation risk measures and further investigations. These site effects can be of great impact on seismic wave amplification and they could thus cause an increment in damage to the structures and cultural-archaeological heritage.

The present study identifies five classes of seismic homogenous microzones, including unstable zones, stable zones prone to local amplification, and stable zones.

The unstable zones are mainly localized in the southern and western sectors of the ancient city (*Insulae meridionalis* and *occidentalis*). In these zones, all the buildings located close to (or directly on) the scarps of the ancient paleocliff and/or are found on significant CT thickness (>5 m) are more susceptible to strong amplification of the seismic wave velocity, as is well documented given the strong damage suffered after the 62–63 AD earthquake.

The stable zones prone to local amplifications are localized in correspondence to ancient paleomorphologies (scarps, ridges, impluvium, steep slopes, and peaks) and/or present greater CT thicknesses. All the buildings included in these zones and/or those found on non-uniform CT thicknesses are also susceptible to be interested by local amplifications, as shown by the great restoration works after the 62–63 AD earthquakes. On the contrary, several sectors of the ancient city can be less susceptible because of not being directly conditioned by local factors and for this reason considered as stable zones.

Finally, the present study points out several sectors of the ancient town where further investigations are needed at second and third levels of SMZ.

Author Contributions: Conceptualization, V.A. and M.C.; methodology, V.A. and M.C.; validation, V.A., M.C., H.D. and A.S.; investigation, V.A. and M.C.; writing—original draft preparation, V.A. and M.C.; writing—review and editing, V.A., M.C., H.D. and A.S. All authors have read and agreed to the published version of the manuscript.

Funding: This research received no external funding.

Data Availability Statement: Not applicable.

Acknowledgments: The authors are grateful to the Officials of the Pompeii Archeological Park, especially to the M. Osanna and G. Zuchtriegel and the V. Amoretti, the Laboratorio di Ricerche Applicate. Thanks also to L. Fornaciari from the Salerno University for the support in elaborating the DTM of the Archaeological Park, to A. Montabert for Figure 2, and to S. Perozzo for the linguistic revision. Finally, the authors are grateful to the three anonymous reviewers for the useful suggestions that helped us to improve the paper.

Conflicts of Interest: The authors declare no conflict of interest.

References

1. Baratta, M. *La Catastrofe sismica calabro-messinese*: *28 dicembre 1908*; Società Geografica Italiana: Bologna, Italy, 1910.
2. Medvedev, S.V. *Engineering Seismology*; Israel Program to Scientific Translations Ltd.: Jerusalem, Israel, 2008; pp. 1–245.
3. Faccioli, E. *Elementi per una guida alle indagini di microzonazione sismica*; Consiglio Nazionale delle Ricerche: Rome, Italy, 1986; pp. 1–146.
4. Kramer, S.L. *Geotechnical Earthquake Engineering*; Prentice Hall: Upper Saddle River, NJ, USA, 1996, pp. 1–567.
5. BSSC NEHRP. *Recommended Provisions for Seismic Regulations for New Buildings and Other Structures*; FEMA Rep. 368, 369; Building Seismic Safety Council for the Federal Emergency Management Agency: Washington, DC, USA, 2000.
6. *EN 1998-1*; Eurocode 8: Design of Structures for Earthquake Resistance. Part 1: General Rules, Seismic Actions and Rules for Buildings. Brussels, Belgium, 2004.
7. Foti, S.; Hollender, F.; Garofalo, F.; Albarello, D.; Asten, M.; Bard, P.Y.; Comina, C.; Cornou, C.; Cox, B.; Di Giulio, G.; et al. Guidelines for the good practice of surface wave analysis: A product of the InterPACIFIC project. *Bull. Earthq. Eng.* **2017**, *16*, 2367–2420. https://doi.org/10.1007/s10518-017-0206-7.

8. Caielli, G.; De Franco, R.; Di Fiore, V.; Albarello, D.; Catalano, S.; Pergalani, F.; Cavuoto, G.; Cercato, M.; Compagnoni, M.; Facciorusso, J.; et al. Extensive surface geophysical prospecting for seismic microzonation. *Bull. Earthq. Eng.* **2020**, *18*, 5475–5502. https://doi.org/10.1007/s10518-020-00866-4.
9. Ansal, A.; Biro, Y. Seismic microzonation: A case study. In *Recent Advanced in Earthquake Geotechnical Engineering and Microzonation*; Kluwer Academic Publishers: Dordrecht, The Netherlands, 2004, pp. 1–234.
10. Kienzle, A.; Hannich, D.; Wirth, W.; Ehret, D.; Rohn, J.; Ciugudean, V.; Czurda, K. A GIS-based study of earthquake hazard as a tool for the microzonation of Bucharest. *Eng. Geol.* **2007**, *87*, 13–32.
11. Mohanty, W.K.; Walling, M.Y.; Nath, S.K.; Pal, I. First Order Seismic Microzonation of Delhi, India Using Geographic Information System (GIS). *Nat. Hazards* **2007**, *40*, 245–260. https://doi.org/10.1007/s11069-006-0011-0.
12. Motamed, R.; Ghalandarzadeh, A.; Tawhata, I.; Tabatabaei, S. Seismic Microzonation and Damage Assessment of Bam City, Southeastern Iran. *J. Earth. Eng.* **2017**,*11*, 388–405. https://doi.org/10.1080/13632460601123164.
13. Ganapathy, G.P.; Rajarathnam, S. Zonation for Seismic Geotechnical Hazard in UrbanAreas—A Case Study Chennai City, India. *Int. J. Earth Sci. Eng.* **2011**, *4*, 436–442.
14. Aucelli, P.P.C.; Di Paola, G.; Valente, E.; Amato, V.; Bracone, V.; Cesarano, M.; Di Capua, G.; Scorpio, V.; Capalbo, A.; Pappone, G.; et al. First assessment of the local seismic amplification susceptibility of the Isernia Province (Molise Region, Southern Italy) by the integration of geological and geomorphological studies related to the first level seismic microzonation project. *Environ. Earth Sci.* **2011**, *77*, 118. https://doi.org/10.1007/s12665-018-7319-4.
15. WGSM (Working Group on Seismic Microzoning). *Indirizzi e criteri per la microzonazione sismica*; Conferenza delle Regioni e delle Province autonome; Dipartimento della Protezione Civile: Rome, Italy, 2008. Available online: https://www.protezionecivile.gov.it/it/pubblicazione/indirizzi-e-criteri-la-microzonazione-sismica (accessed on 11 June 2020).
16. WGSMLA (Working Group on Seismic Microzoning the L'Aquila Area). *Microzonazione sismica per la ricostruzione dell'area aquilana*; Dipartimento della Protezione Civile: Regione Abruzzo, Italy, 2010; 3 vols. and DVD. Available online: https://centromicrozonazionesismica.it/en/download-en/category/11-microzonazione-sismica-per-la-ricostruzione-dell-area-aquilana (accessed on 11 June 2021). (In Italian)
17. AA.VV. Contributi per l'aggiornamento degli "Indirizzi e criteri per la microzonazione sismica". *Ingegneria Sismica* **2011**, *28*, 16–26. Available online: https://www.centromicrozonazionesismica.it/it/download/category/17-contributi-per-l-aggiornamento-degli-indirizzi-e-criteri-per-la-microzonazione-sismica (accessed on 11 June 2021). (In Italian)
18. CTMS (Commissione tecnica per la Microzonazione sismica). *Standard di Rappresentazione ed archiviazione informatica*; Department of Civil Protection: Rome, Italy, 2011. Available online: https://www.webms.it/sites/default/files/2018-06/StandardMS_4_1.pdf (accessed on 11 June 2021).
19. ASTM. *Standard Practice for Classification of Soils for Engineering Purposes* (*Unified Soil Classification System*); ASTM International: West Conshohocken, PA, USA, 2011. Available online: https://lauwtjunnji.weebly.com/uploads/1/0/1/7/10171621/astm_d-2487_classification_of_soils_for_engineering_purposes_unified_soil_classification_system.pdf (accessed on 22 June 2021).
20. Amanti, M.; Chiessi, V.; Muraro, C.; Puzzilli, L.M.; Roma, M.; Catalano, S.; Romagnoli, G.; Tortorici, G.; Cavuoto, G.; Albarello, D.; et al. Geological and geotechnical models definition for 3rd level seismic microzonation studies in Central Italy. *Bull. Earthq. Eng.* **2020**, *18*, 5441–5473. https://doi.org/10.1007/s10518-020-00843-x.
21. Ciancimino, A.; Lanzo, G.; Alleanza, G.A.; Amoroso, S.; Bardotti, R.; Biondi, G.; Cascone, E.; Castelli, F.; Di Giulio, A.; D'Onofrio, A.; et al. Dynamic characterization of fine-grained soils in Central Italy by laboratory testing. *Bull. Earthq. Eng.* **2020**, *18*, 5503–5531. https://doi.org/10.1007/s10518-019-00611-6.
22. Pagliaroli, A.; Pergalani, F.; Ciancimino, A.; Chiaradonna, A.; Compagnoni, M.; De Silva, F.; Foti, S.; Giallini, S.; Lanzo, G.; Lombardi, F.; et al. Site response analyses for complex geological and morphological conditions: Relevant case-histories from 3rd level seismic microzonation in Central Italy. *Bull. Earthq. Eng.* **2020**, *18*, 5741–5777. https://doi.org/10.1007/s10518-019-00610-7.
23. Cinque, A.; Irollo, L. Il "Vulcano di Pompei": Nuovi dati geomorfologici e stratigrafici. *Il Quat. Ital. J. Quat. Sci.* **2004**, 17, 101–116.
24. Silva, P.G.; Borja, F.; Zazo, C.; Goy, J.L.; Bardají, T.; De Luque, L.; Lario, J.; Dabrio, C.J. Archaeoseismic record at the ancient Roman city of Baelo Claudia (Cádiz, south Spain). *Tectonophysics* **2005**, *408*, 129–146. https://doi.org/10.1016/j.tecto.2005.05.031.
25. Ambraseys, N.N. Earthquakes and archaeology. *J. Archaeol. Sci.* **2006**, *33*, 1008–1016. https://doi.org/10.1016/j.jas.2005.11.006.
26. Caputo, R.; Helly, B.; Pavlides, S.; Papadopoulos, G. Archaeo- and palaeoseismological investigations in Northern Thessaly (Greece): Insights for the seismic potential of the region. *Nat. Hazards* **2006**, *39*, 195–212. https://doi.org/10.1007/s11069-006-0023-9.
27. Karakhanyan, A.; Avagyan, A.; Sourouzian, H. Archaeoseismological studies at the temple of Amenhotep III, Luxor, Egypt. *Geol. Soc. Am. Bull.* **2010**, *471*, 199–222. https://doi.org/10.1130/2010.2471(17).
28. Sintubin, M. Archaeoseismology: Past, present and future. *Quat. Int.* **2011**, *242*, 4–10. https://doi.org/10.1016/j.quaint.2011.03.056.
29. Jusseret, S. Earthquake archaeology: A future in ruins? *J. Chromatogr.* **2014**, *A1*, 277–296. https://doi.org/10.1558/jca.v1i2.20487.
30. Despotaki, V.; Silva, V.; Lagomarsino, S.; Pavlova, I.; Torres, J. Evaluation of seismic risk on UNESCO cultural heritage sites in Europe. *Int. J. Archit. Herit.* **2018**, *12*, 1231–1244. https://doi.org/10.1080/15583058.2018.1503374.
31. Pecchioli, L.; Cangi, G.; Marra, F. Evidence of seismic damages on ancient Roman buildings at Ostia: An arch mechanics approach. *J. Archaeol. Sci. Rep.* **2018**, *21*, 117–127. https://doi.org/10.1016/j.jasrep.2018.07.006.

32. Brando, G.; Cocco, G.; Mazzanti, C.; Peruch, M.; Spacone, E.; Alfaro, C.; Sovero, K.; Tarque, N. Structural survey and empirical seismic vulnerability assessment of dwellings in the historical centre of Cusco, Peru. *Int. J. Archit. Herit.* **2019**, *13*, 1–29. https://doi.org/10.1080/15583058.2019.1685022.
33. Davis, C.; Coningham, R.; Acharya, K.P.; Kunwar, R.B.; Forlin, P.; Weise, K.; Maskey, P.N.; Joshi, A.; Simpson, I.; Toll, D.; et al. Identifying archaeological evidence of past earthquakes in a contemporary disaster scenario: Case studies of damage, resilience and risk reduction from the 2015 Gorkha Earthquake and past seismic events within the Kathmandu Valley UNESCO World Heritage Property (Nepal). *J. Seismol.* **2020**, *24*, 729–751. https://doi.org/10.1007/s10950-019-09890-7.
34. Dessales, H. (Ed.) *The Villa of Diomedes, the Making of a Roman Villa in Pompeii*, 1st ed.; Hermann: Paris, France; Centre Jean Bérard: Naples, Italy, 2020.
35. Montabert, A.; Dessales, H.; Arrighetti, A.; Clément, J.; Lancieri, M.; Lyon-Caen, H. Tracing the seismic history of Sant'Agata del Mugello (Italy, Tuscany) through a cross-disciplinary approach. *J. Archaeol. Sci. Rep.* **2020**, *33*, 102440. https://doi.org/10.1016/j.jasrep.2020.102440.
36. Combey, A.; Tricoche, A.; Audin, L.; David, G.; Benavente Escóbar, C.; Abuhadba, J.; Tavera, H.; Rodriguez-Pascua, M. Monumental Inca remains and past seismic disasters: A relational database to support archaeoseismological investigations and cultural heritage preservation in the Andes. *J. S. Am. Earth Sci.* **2021**, *111*, 103447. https://doi.org/10.1016/j.jsames.2021.103447.
37. Montabert, A. Characterizing Ground Motion of Historical Earthquackes. Study of Sant'Agata del Mugello Combining Building Archeology, Earthquake Engineering and Seismology. Ph.D. Thesis, Ecole Normal Superieure, Paris, France, 2021.
38. Adam, J.P. Observations techniques sur les suites du séisme de 62 à Pompéi. In *Tremblement de terre, éruptions volcaniques et vie des hommes dans la Campanie antique*, 1st ed.; Albore Livadie, C., Ed.; Centre Jean Bérard: Rome, Italy, 1986; pp. 67–87.
39. Zevi, F. Il terremoto del 62 e l'edilizia privata pompeiana. In *Pompei*, 1st ed.; Zevi, F., Eds.; Banco di Napoli: Naples, Italy, 1992; Volume II, pp. 39–58.
40. Allison, P. On-going seismic activity and its effects on the living conditions in Pompeii in the last decades. In *Archäologie und Seismologie. La Regione Vesuviana dal 62 al 79 d.C. Problemi archeologici e sismologici. Colloquium di Boscoreale, 26–27 novembre 1993*, 1st ed.; DAI. Römische Abteilung., Soprintendenza Archeologica di Pompei, Osservatorio vesuviano, Eds.; Biering & Brinkmann: München, Germany, 1995; pp. 183–190.
41. De Simone, A. I terremoti precedenti l'eruzione. Nuove attestazioni da recenti scavi. In *Archäologie und Seismologie. La Regione Vesuviana dal 62 al 79 d.C. Problemi archeologici e sismologici. Colloquium di Boscoreale, 26–27 novembre 1993*, 1st ed.; DAI. Römische Abteilung., Soprintendenza Archeologica di Pompei., Osservatorio vesuviano, Eds.; Biering & Brinkmann: München, Germany, 1995; pp. 37–43.
42. Jacobelli, L. I terremoti fra il 62 e il 79 nell'area vesuviana: Le ragioni di un convegno. In *Archäologie und Seismologie. La Regione Vesuviana dal 62 al 79 d.C. Problemi archeologici e sismologici. Colloquium di Boscoreale, 26–27 novembre 1993*, 1st ed.; DAI. Römische Abteilung., Soprintendenza Archeologica di Pompei., Osservatorio vesuviano, Eds.; Biering & Brinkmann: München, Germany, 1995; pp. 17–21.
43. Ling, R. Earthquake danahe in Pompeii I 10: One earthquake or two. In *Archäologie und Seismologie. La Regione Vesuviana dal 62 al 79 d.C. Problemi archeologici e sismologici. Colloquium di Boscoreale, 26–27 novembre 1993*, 1st ed.; DAI. Römische Abteilung., Soprintendenza Archeologica di Pompei., Osservatorio vesuviano, Eds.; Biering & Brinkmann: München, Germany, 1995; pp. 201–209.
44. Nappo, S.C. Evidenze di danni strutturali, restauri e rifacimenti nelle insulae gravitanti su Via Nocera a Pompei. In *Archäologie und Seismologie. La Regione Vesuviana dal 62 al 79 d.C. Problemi archeologici e sismologici. Colloquium di Boscoreale, 26–27 novembre 1993*, 1st ed.; DAI. Römische Abteilung., Soprintendenza Archeologica di Pompei., Osservatorio vesuviano, Eds.; Biering & Brinkmann: München, Germany, 1995; pp. 45–55.
45. Pappalardo, U. Osservazioni su un secondo grande terremoto a Pompei. In *Archäologie und Seismologie. La Regione Vesuviana dal 62 al 79 d.C. Problemi archeologici e sismologici. Colloquium di Boscoreale, 26–27 novembre 1993*, 1st ed.; DAI. Römische Abteilung., Soprintendenza Archeologica di Pompei., Osservatorio vesuviano, Eds.; Biering & Brinkmann: München, Germany, 1995; pp. 191–194.
46. Renna, E. La realtà sismologica dell'area vesuviana prima e dopo il 79 d.C. attraverso l'analisi delle fonti antiche. In *Archäologie und Seismologie. La Regione Vesuviana dal 62 al 79 d.C. Problemi archeologici e sismologici. Colloquium di Boscoreale, 26–27 novembre 1993*, 1st ed.; DAI. Römische Abteilung., Soprintendenza Archeologica di Pompei., Osservatorio vesuviano, Eds.; Biering & Brinkmann: München, Germany, 1995; pp. 195–199.
47. Staub-Gierow, M. Indizien für ein zweites Erdbeben? Beobachtungen in der Casa del Granduca (VII 4, 56) un der Casa dei Capitelli Figurati (VII 4, 57) in Pompeji. In *Archäologie und Seismologie. La Regione Vesuviana dal 62 al 79 d.C. Problemi archeologici e sismologici. Colloquium di Boscoreale, 26–27 novembre 1993*, 1st ed.; DAI. Römische Abteilung., Soprintendenza Archeologica di Pompei., Osservatorio vesuviano, Eds.; Biering & Brinkmann: München, Germany, 1995; pp. 67–74.
48. Varone, A. Più terremoti a Pompei? I nuovi dati degli scavi di Via dell'Abbondanza. In *Archäologie und Seismologie. La Regione Vesuviana dal 62 al 79 d.C. Problemi archeologici e sismologici. Colloquium di Boscoreale, 26–27 novembre 1993*, 1st ed.; DAI. Römische Abteilung., Soprintendenza Archeologica di Pompei., Osservatorio vesuviano, Eds.; Biering & Brinkmann: München, Germany, 1995; pp. 29–35.
49. Varone, A. Convivere con i terremoti. La travagliata ricostruzione di Pompei dopo il terremoto del 62 d.C. In *Omni pede stare. Saggi architettonici e circumvesuviani in memoriam Jos de Waele*, 1st ed.; Studi della Soprintendenza Archeologica di Pompei, 9; Mols, S.T.A., Moormann, E.M., Eds.; Electa: Naples, Italy; pp. 315–323.

50. Covolan, M. Tra *utilitas*, *distributio* e *perpetuitas*: l'impiego del tufo giallo napoletano nell'edilizia pompeiana; Santoriello, A., Dessales, H., tutors. Ph.D. Thesis, Università degli Studi di Salerno, Salerno, Italy, 2021.
51. Dessales, H. (Ed.) *Ricostruire dopo un terremoto. Riparazioni antiche a Pompei*; Centre Jean Bérard: Naples; Italy, 2022.
52. Dessales, H. Construction et culture sismique à l'époque romaine. *Ædificare* **2020**, *7*, 45–76. https://doi.org/10.15122/isbn.978-2-406-11428-4.
53. Di Vito, M.A.; Sulpizio, R.; Zanchetta, G.; Calderoni, G. The geology of the South Western Slope of Somma-Vesuvius, Italy, as inferred by borehole stratigraphies and cores. *Acta Vulcanol.* **1998**, *10*, 383–397.
54. Amato, V. L'approccio geoarcheologico per la ricostruzione crono-stratigrafica del sottosuolo di Pompei: l'esempio dei saggi di scavo all'Insula dei Casti Amanti. In *Ricerche e scoperte a Pompei: In ricordo di Enzo Lippolis*; Osanna, M., ed.; Studi della Soprintendenza Archeologica Pompei, 45; L'Erma di Bretschneider: Rome, Italy, 2021; pp. 117–130.
55. Amato, V.; Aiello, G.; Barra, D.; Infante, A.; Di Vito, M. Nuovi dati geologici per la ricostruzione degli ambienti marino-costieri del 79 d.C. a Pompeii. *RStPomp* **2021**, *XXXII*, 103–111.
56. Di Girolamo, P. La serie piroclastica dell'eruzione di Pompei, studio chimico–petrografico, mineralogico e stratigrafico dell'eruzione del 79 d.C. e dei prodotti ottavianitici del Somma-Vesuvio. *Ann. Oss. Ves.* **1963**, *V*, 1–69.
57. Di Girolamo, P. Un esempio di lava schiuma (foam lava) in Campania. (lava schiuma di Pompei scavi). *Rend. Acc. Sci. Fis. Mat. Napoli* **1968**, XXXV, 3–12.
58. Senatore, M.R.; Ciarallo, A.; Stanley, J. Pompeii damaged by volcaniclastic debris flows triggered centuries prior to the 79 A.D. Vesuvius eruption. *Geoarchaeology* **2014**, *29*, 1–15.
59. Savino, E. Nerone, Pompei e il terremoto del 63 d.C. In *Interventi imperiali in campo economico e sociale*: *Da Augusto al tardoantico*, 1st ed.; Merola, G.D., Ed.; Edipuglia: Bari, Italy, 2009; pp. 225–244.
60. Marturano, A.; Rinaldis, V. Seismicity before the 79 A.D. Vesuvius eruption. In *Il sistema uomo-abiente tra passato e presente*, 1st ed.; Albore Livadie, C., Ortolani, F., Eds.; Territorio storico e ambiente, 1; Edipuglia: Bari, Italy, 1998; pp. 237–246.
61. Cubellis, E.; Luongo, G.; Marturano, A. Seismic hazard assessment at Mt. Vesuvius: Maximum expected magnitude. *J. Volcanol. Geotherm. Res.* **2007**, *118*, 339–351. https://doi.org/10.1016/j.jvolgeores.2007.03.003.
62. Guidoboni, E.; Ferrari, G.; Mariotti, D.; Comastri, A.; Tarabusi, G.; Sgattoni., G.; Valensise, G. CFTI5Med. In *Catalogo dei Forti Terremoti in Italia* (*461 a.C.-1997*) *e nell'area Mediterranea* (*760 a.C.-1500*); Istituto Nazionale di Geofisica e Vulcanologia (INGV): Naples, Italy, 2018. Available online: http://storing.ingv.it/cfti/cfti5 (accessed on 20 July 2020).
63. Guidoboni, E.; Ferrari, G.; Tarabusi, G.; Sgattoni, G.; Comastri, A.; Mariotti, D.; Ciuccarelli, C.; Bianchi, M.G.; Valensise, G. CFTI5Med, the new release of the catalogue of strong earthquakes in Italy and in the Mediterranean area. *Sci. Data* **2019**, *6*, 1–15. https://doi.org/10.1038/s41597-019-0091-9.
64. Amato, V.; Giletti, F. Dalle origini del paesaggio pompeiano alla città di Pompei. *RSTPomp* **2022**, *XXXIII*, 103–111. (In Italian)
65. Strocka, V.M. *Casa del Principe di Napoli* (*VI 15*, *7.8*), 1st ed.; Häusern in Pompeji, 1; Hirmer: München, Germany, 1984.
66. Ehrhardt, W. *Casa dell'orso* (*VII 2*, *44–46*), 1st ed.; Häusern in Pompeji, 2; Hirmer: München, Germany, 1988.
67. Michel, D. *Casa dei Cei* (*I 6*, *5*), 1st ed.; Häusern in Pompeji, 3; Hirmer: München, Germany, 1990.
68. Strocka, V.M. *Casa del Labirinto* (*VI 8*, *10*), 1st ed.; Häusern in Pompeji, 4; Hirmer: München, Germany, 1991.
69. Seiler, F. *Casa degli amorini dorati* (*VI 16*, *7.38*), 1st ed.; Häusern in Pompeji, 5; Hirmer: München, Germany, 1992.
70. Stemmer, K. *Casa dell'ara massima* (*VI 16*, *15–17*), 1st ed.; Häusern in Pompeji, 6; Hirmer: München, Germany, 1992.
71. Staub Gierow, M. *Casa del Granduca* (*VII 4*, *56*), *Casa dei Capitelli figurati* (*VII 4*, *57*), 1st ed.; Häusern in Pompeji, 7; Hirmer: München, Germany,1994.
72. Frölich, T. *Casa della fontana piccola* (*VI 8*, *23–24*), 1st ed.; Häusern in Pompeji, 8; Hirmer: München, Germany, 1996.
73. Ehrhardt, W. *Casa di Paquius Proculus* (*I 7*, *1.20*), 1st ed.; Häusern in Pompeji, 9; Hirmer: München, Germany, 1998.
74. Staub Gierow, M. *Casa della parete nera* (*VII 4*, *58–60*), *Casa delle Forme di Creta* (*VII 4*, *61–63*), 1st ed.; Häusern in Pompeji, 10; Hirmer: München, Germany, 2000.
75. Allison, P.M.; Sear, F.B. *Casa della caccia antica* (*VII 4*, *48*), 1st ed.; Häusern in Pompeji, 11; Hirmer: München, Germany, 2002.
76. Ehrhardt, W. *Casa delle nozze d'argento* (*V 2*, *i*), 1st ed.; Häusern in Pompeji, 12; Hirmer: München, Germany, 2004.
77. Coarelli, F.; Pesando, F. (Eds.); *Rileggere Pompei*, *I. L'*insula *10 della* Regio *VI*; Studi della Soprintendenza Archeologica Pompei, 12; L'Erma di Bretschneider: Rome, Italy, 2006.
78. Verzár-Bass, M.; Flaviana, O. (Eds.); *Rileggere Pompei*, *II 2. L'insula 13 della* Regio *VI*; Studi della Soprintendenza Archeologica Pompei, 30; L'Erma di Bretschneider: Rome, Italy, 2010.
79. Pesando, F.; Giglio, M. (Eds.); *Rileggere Pompei*, *V. L'insula 7 della Regio IX*; Studi della Soprintendenza Archeologica Pompei, 36; L'Erma di Bretschneider: Rome, Italy, 2017.
80. Zaccaria Ruggiu, A.P.; Maratini, C. (Eds.); *Rileggere Pompei*, *IV. L'insula 7 della Regio VI*; Studi della Soprintendenza Archeologica Pompei, 35; L'Erma di Bretschneider: Rome, Italy, 2017.
81. Anderson, M.; Robinson, D. (Eds.); *House of Surgeon, Pompeii: Excavations in the Casa del Chirurgo* (*VI 1*, *9–10.23*), 1st ed.; Oxbow Books: Oxford, UK, 2018.
82. Bragantini, I.; De Vos, M.; Parise Badoni, F.; Sampaolo, V. *2. Regioni V*, *VI*. Pitture e pavimenti di Pompei, 2; Ministero per I beni culturali e ambientali, ICCD: Rome, Italy, 1983.
83. AA.VV. IV. Regio VI, parte prima. In *Pompei: Pitture e Mosaici, 4*; Istituto dell'Enciclopedia Italiana: Rome, Italy, 1993.
84. Coarelli, F.; Zaccaria Ruggiu, A.P.; Pesando, F.; Branconi, P. Pompei: "Progetto *Regio* VI". Relazione preliminare degli scavi nelle insulae 10 e 14. *RStPomp* **2003**, *XII–XIII*, 221–228.

85. Cassetta, R.; Costantino, C. La Casa del Naviglio (VI 10,11) e le botteghe VI 10,10 e VI 10,12. In *Rileggere Pompei, I. L'insula 10 della Regio VI*, 1st ed.; Coarelli, F., Pesando, F., Eds.; Studi della Soprintendenza Archeologica Pompei, 12; L'Erma di Bretschneider: Rome, Italy, 2006; pp. 243–336.
86. Zanella, S. Pompei. Sulle tracce di fondazione e rifondazioni urbane. *R. St. Pomp.* **2020**, *XXX*, 7–21.
87. Maiuri, A. *L'ultima fase edilizia di Pompei*; 1942. Reprinted by Pesando, F., Ed.; Associazione Internazionale Amici di Pompei: Naples, Italy, 2002
88. Bragantini, 3. *Regioni VII, VIII, IX.*; *Indici delle regioni I–IX*; Pitture e pavimenti di Pompei, 3; Ministero per i beni culturali e ambientali, ICCD: Rome, Italy, 1986.
89. Favicchio, C. *I danni del terremoto del 62 d.C. a Pompei nella* Regio *VIII*: *Metodo di ricerca e scoperte*, 1st ed.; Libreria l'Ateneo: Naples, Italy, 1996.
90. AA.VV. VIII. Regio VIII e Regio IX parte prima. In *Pompei: Pitture e Mosaici, 8*; Istituto dell'Enciclopedia Italiana: Rome, Italy, 1998.
91. Giacobello, F. *Larari pompeiani*: *Iconografia e culto dei Lari in ambito domestico*, 1st ed.; Il Filarete: Milan, Italy, 2008.
92. Mazois, F. *Les Ruines de Pompéi, dessinées et mesurées par F. Mazois, pendant les années MDCCCIX, MDCCCX, MDCCCXI*, 1st ed.; Imprimerie et librairie de Firmin Diderot: Paris, France, 1824.
93. AA.VV. VI. Regiones VI parte terza e VII parte prima. In *Pompei: Pitture e Mosaici, 6*; Istituto dell'Enciclopedia Italiana: Rome, Italy, 1996.